Geol. Mag. **143** (*3*), *2006, pp. 367–391. © 2006 Cambridge University Press*
doi:10.1017/S0016756805001640 *Printed in the United Kingdom*

Provenance of north Gondwana Cambrian–Ordovician sandstone: U–Pb SHRIMP dating of detrital zircons from Israel and Jordan

K. KOLODNER*†, D. AVIGAD*, M. MCWILLIAMS‡, J. L. WOODEN§, T. WEISSBROD¶ & S. FEINSTEIN||

Institute of Earth Sciences, The Hebrew University of Jerusalem, Jerusalem 91904, Israel
Geological & Environmental Sciences, Stanford University, Stanford, California 94305-2115, USA
U.S Geological Survey, Menlo Park, California 94025, USA
Geological Survey of Israel, 30 Malchai-Israel St., Jerusalem 95501, Israel
Departments of Geological and Environmental Sciences, Ben Gurion, University of the Negev 84105, Israel

(*Received* 21 February 2005; *accepted* 25 August 2005)

Abstract – A vast sequence of quartz-rich sandstone was deposited over North Africa and Arabia during Early Palaeozoic times, in the aftermath of Neoproterozoic Pan-African orogeny and the amalgamation of Gondwana. This rock sequence forms a relatively thin sheet (1–3 km thick) that was transported over a very gentle slope and deposited over a huge area. The sense of transport indicates unroofing of Gondwana terranes but the exact provenance of the siliciclastic deposit remains unclear. Detrital zircons from Cambrian arkoses that immediately overlie the Neoproterozoic Arabian–Nubian Shield in Israel and Jordan yielded Neoproterozoic U–Pb ages (900–530 Ma), suggesting derivation from a proximal source such as the Arabian–Nubian Shield. A minor fraction of earliest Neoproterozoic and older age zircons was also detected. Upward in the section, the proportion of old zircons increases and reaches a maximum (40 %) in the Ordovician strata of Jordan. The major earliest Neoproterozoic and older age groups detected are 0.95–1.1, 1.8–1.9 and 2.65–2.7 Ga, among which the 0.95–1.1 Ga group is ubiquitous and makes up as much as 27 % in the Ordovician of Jordan, indicating it is a prominent component of the detrital zircon age spectra of northeast Gondwana. The pattern of zircon ages obtained in the present work reflects progressive blanketing of the northern Arabian–Nubian Shield by Cambrian–Ordovician sediments and an increasing contribution from a more distal source, possibly south of the Arabian–Nubian Shield. The significant changes in the zircon age signal reflect many hundreds of kilometres of southward migration of the provenance.

Keywords: zircon, Cambrian–Ordovician, Arabian–Nubian Shield, provenance.

1. Introduction

A widespread sedimentary platform, essentially comprising quartz-rich sandstone, was deposited over the continental margins of North Africa and Arabia during the Early Palaeozoic times, in the aftermath of the Neoproterozoic amalgamation of Gondwana. This sedimentary succession is unique in several aspects: (1) it is one of the most voluminous siliciclastic sequences ever deposited on a continental crust (Burke & Kraus, 2000); (2) in spite of its great volume it forms a rather thin cover on top of the (then) recently stabilized East Sahara craton and the Arabian–Nubian Shield; (3) it is made essentially of quartz, and it was deposited from a continental-wide braided stream system with a constant south-to-north (present configuration) flow direction over a very gentle slope (Fig. 1; McKee, 1962; Klitzsch, 1981; Klitzsch *et al.* 1979; T. Weissbrod, unpub. Ph.D. thesis, Hebrew Univ. Jerusalem, 1980; Alsharhan & Nairn, 1997; Burke & Kraus, 2000; Burke, MacGregor & Cameron, 2003). The successions across North Africa and the Middle East form part of a continuous platform that was deposited on a very broad and nearly flat continental basement shortly after the wearing down of the Pan-African orogen. The significant volume of detrital quartz stored in the platform sequences indicates a major phase of continental denudation and basement unroofing. Burke, MacGregor & Cameron (2003) envisaged Cambrian sedimentation in relation to rifting and thermal subsidence, but we note that the majority of the Cambrian–Ordovician sediments in North Africa and Arabia were deposited as thin and laterally widespread rock sheets. Previous workers emphasized that the Cambrian–Ordovician sediments differ significantly from the typically much thicker and narrower rift-related continental margin deposits and Bennacef *et al.* (1971) named the early Palaeozoic sandstone of Algerian Sahara 'Cratonic sediments'. In the northern Arabian–Nubian Shield, extension and incipient rifting has locally affected the collapsing Pan-African orogen, but the field and geochronological data indicate that the extensional basins were formed by 600–580 Ma

† Author for correspondence: kerenk@vms.huji.ac.il

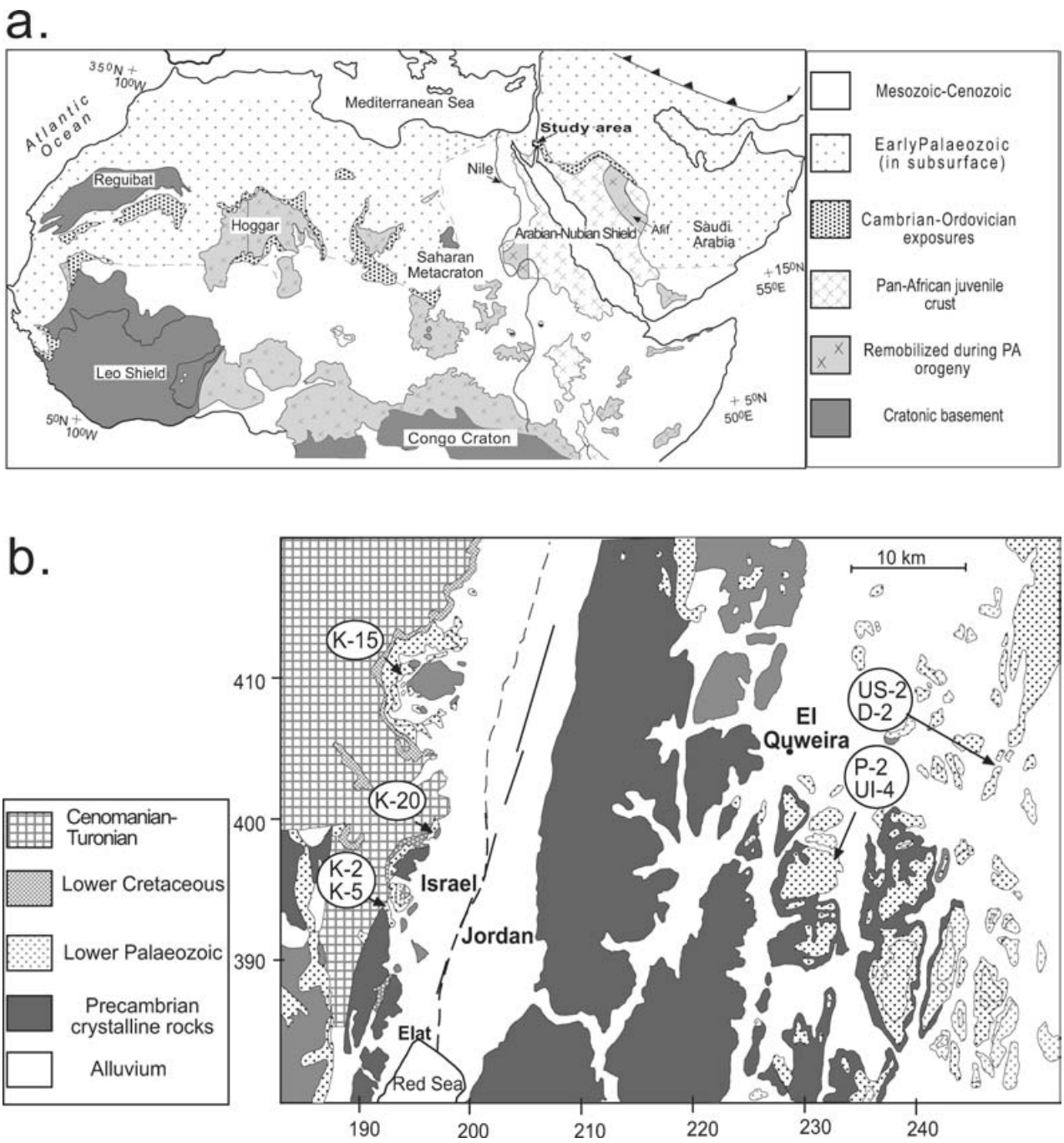

Figure 1. Simplified geological and location maps. (a) Geological map of Northeast Africa and Arabia showing exposures of the Precambrian rocks and Palaeozoic sediments, including the study areas in southern Israel and southern Jordan (after Avigad *et al.* 2003). (b) Generalized geological map of southern Israel and southern Jordan, International Grid coordinates (after Bentor *et al.* 1987). The map shows the geological rock units and the sample locations of the Cambrian samples in Israel and the Cambrian and Ordovician samples in Jordan.

(Jarrar, Wachendorf & Zellmer, 1991; Willis, Stern & Clauer, 1988; Johnson, 2003), well before the onset of Cambrian sedimentation. By Cambrian–Ordovician times, these extensional basins, together with their host basement, were sealed and covered by the sandstone blanket that spread far from any known rift.

The stratigraphy and depositional environment of the Cambrian–Ordovician platform sequence has been studied extensively (e.g. T. Weissbrod, unpub. Ph.D. thesis, Hebrew Univ. Jerusalem, 1980; Weissbrod & Nachmias, 1986; Gaudette & Hurley, 1979; Amireh, 1991; Alsharhan & Nairn, 1997; Garfunkel, 2002; Wolfart, 1981; Petters, 1991 and references therein), but details such as the scale of detrital transport and the nature of the provenance are not well understood. Several papers have interpreted the provenance of the

siliciclastic sections in North Africa and Arabia using petrography, petrology and geochronology. Weissbrod (1969; T. Weissbrod, unpub. Ph.D. thesis, Hebrew Univ. Jerusalem, 1980) and Weissbrod & Nachmias (1986) suggested that most of the sandstone shares a common provenance, and that facies distribution throughout the sedimentary column points to the Arabian–Nubian mainland in the south as the area of sediment supply. Karcz & Key (1966) and Selley (1972) showed that palaeocurrent data from southern Israel and Jordan indicate transport direction towards the northwest or northeast, and Powell (1989) argued that the siliciclastics of Jordan were derived from a distant source to the south. Garfunkel (1999, 2002) suggested that the area of deposition gradually expanded, from a width of 100 km in the Early Cambrian to well over 1000 km in the Ordovician and Silurian. The constant north-to-south directed transport of detritus, as deduced from field sedimentological criteria, is an important line of evidence indicating the provenance was south of the deposition site of any given sandstone outcrop, yet the great width of the sedimentary blanket, from the Mediterranean shoreline in the north, far inland to Chad and Yemen in the south (Fig. 1), allows derivation from a variety of 'southerly' sources.

The Cambrian–Ordovician sandstone sequence, which includes deposits in Israel and Jordan, covers the northern outskirts of the East African Orogen. The East African Orogen is a Neoproterozoic orogenic belt that stretches from Mozambique in the south to Israel and Jordan in the north (Stern, 1994). In the north, the East African Orogen comprises the Arabian–Nubian Shield, which is made of accreted Neoproterozoic (900–550 Ma) juvenile volcanic arcs (Bentor, 1985; Stern, 1994), while to the south, the East African Orogen comprises the Mozambique belt, which is a broad suture zone encompassing ancient crust remobilized during Neoproterozoic times (Stern, 1994 and references therein). The entire length of the East African Orogen was unroofed in the aftermath of Pan-African orogeny. Much of the upper crust has been removed from above the Arabian–Nubian shield to expose late Neoproterozoic greenschist-facies metamorphic rocks typical to this domain (Garfunkel, 1999; Stern, 1994), whereas an even greater depth of exposure is inferred from the abundant granulite- and amphibolite-facies rocks in the Mozambique belt (Stern, 1994). Both terranes were thus likely candidates to shed detritus onto northern Gondwana margins, but the southern parts of the East African Orogen probably drained to the south (currently southern Africa), where Early Palaeozoic sandstones are also widespread (Shackleton, 1986).

Recent U–Pb SHRIMP dating of detrital zircons from the Cambrian succession of southern Israel revealed that most detrital zircons yielded Neoproterozoic ages (Avigad *et al.* 2003), indicating that the Early Palaeozoic siliciclastic section stores detritus shed from the East African Orogen, but pre-Neoproterozoic zircons were also found. Avigad *et al.* (2003) presented a single collective histogram for the entire Cambrian section of Israel. However, the Cambrian section matures upward from arkose and subarkose with pebbly conglomerates at the base, to pure quartz arenite at the top. These mineralogical changes take place over a section less than 300 m thick, and potentially indicate significant differences in transport distances and in provenance. Thus, the histogram presented by Avigad *et al.* (2003) bears on the general nature of the provenance of the Early Palaeozoic of north Gondwana, but it does not clarify the character of the 'cratonic' sedimentation process and whether the provenance has changed with time.

Here, we report U–Pb SHRIMP ages of detrital zircons collected from different stratigraphic levels of the Cambrian section exposed in Israel and from the Cambrian and Ordovician sections exposed in southern Jordan. We present the data from Israel with a finer-scale resolution than that published by Avigad *et al.* (2003) and report the results from each of the four stratigraphic levels of the Cambrian in Israel. We also present detrital zircon U–Pb ages from four Cambrian and Ordovician sandstone samples from strata exposed in southern Jordan. Detrital minerals from these rocks have never been dated. This study covers a relatively broad area and a significant fraction of the early Palaeozoic record, and the stratigraphic control allows detection of the trends and changes in provenance during the Cambrian–Ordovician period.

2. Lower Palaeozoic sedimentary cover

At the end of the Neoproterozoic era, the basement of North Africa and Arabia subsided and widespread deposition of arkose and mature sandstone began at 530–515 Ma (late–early Cambrian) (Alsharhan & Nairn, 1997; Garfunkel, 1999; Klitzsch, 1981; Petters, 1991 and references therein; Wolfart, 1981). The cover sediments evolved on a vast peneplain and the basement was progressively buried as sedimentation gradually transgressed southward (Garfunkel, 1999). Over wide areas of northern Gondwana, including the Middle East (Alsharhan & Nairn, 1997; Klitzsch, 1981; Wolfart, 1981), the Palaeozoic sedimentary history was uniform. In North Africa, fluvial arkose accumulated in the late–early Cambrian (Tomotian–Botomian), followed by subarkose and mature sandstone that accumulated during a marine transgression that progressed from north to south (Klitzsch, 1981). During late Ordovician times, Gondwanaland moved over the south pole, leading to widespread continental glaciations in Africa (Alsharhan & Nairn, 1997; Klitzsch, 1981). Our work has concentrated on sedimentary units deposited prior to this glaciation period (late Ordovician).

2.a. The Cambrian of southern Israel

The Lower Palaeozoic section is exposed in the Elat area, where the Cambrian sucession is about 300 m thick and is unconformably overlain by Cretaceous rocks (Fig. 2; Garfunkel, 1978; T. Weissbrod, unpub. Ph.D. thesis, Hebrew Univ. Jerusalem, 1980). The lower most stratigraphic unit, the Amudei Shelomo Formation, is generally medium- to coarse-grained sub-arkose, with sub-angular to sub-rounded grains. A basal conglomerate consisting of angular to rounded pebbles of magmatic or metamorphic origin is found at the base of the formation (T. Weissbrod, unpub. Ph.D. thesis, Hebrew Univ. Jerusalem, 1980). The overlying Timna Formation displays a mixed siliciclastic (subarkose)–carbonate facies. The lower part of the Shehoret Formation consists of siltstone and shale alternating with fine- to coarse-grained subarkose. These are overlain by a thick, quite homogeneous fine-grained, sub-angular to sub-rounded, moderately sorted subarkose cemented by microcrystalline quartz. The uppermost Netafim Formation is a fine-grained, rounded and well-sorted, quartz-arenite with alternating layers of siltstone and claystone. Heavy minerals are zircon, tourmaline, rutile (ZTR) and ores, with irregular distribution of authigenic apatite and barite (Weissbrod & Nachmias, 1986). The ZTR index (zircon, tourmaline, rutile) in the upper Cambrian rocks is above 90 %, implying significant mineralogical maturation.

2.b. The Cambrian–Ordovician of southern Jordan

East of the Dead Sea Rift, Cambrian cover strata form a ~500 km wide belt stretching from Jordan into Saudi Arabia, whereas Ordovician strata extend further to the south where they commonly lie directly on the basement (Fig. 1; Garfunkel, 2002). The Palaeozoic strata of southern Jordan consist of the Cambrian to Lower Ordovician Ram Group and the Ordovician to Silurian Khreim Group (Powell, 1989). From base to top, the Cambrian succession (Fig. 2) consists of the Salib Formation (coarse arkosic sandstone and pebbly conglomerates), Burj Formation (shallow marine subarkose, dolomite-shale), Umm-Ishrin Formation (mature quartz-arenite) and the lower Disi Formation (mature quartz-arenite) (T. Weissbrod, unpub. Ph.D. thesis, Hebrew Univ. Jerusalem, 1980; Garfunkel, 1999; Amireh, 1991).

The early–middle Ordovician formations, which were examined in this research, consist of alternating cycles of fine- to medium-grained quartz arenite deposited over a shallow shelf of a broad sea (Selley, 1972; Bender, 1974; Powell, 1989, Powell, Moh'd & Masri, 1994).The Lower Ordovician succession is composed of quartz arenites of the upper Disi Formation and the Umm Sahm Formation at the top of the Ram Group. The upper part of the Ordovician succession includes the lower part of the Khreim Group with

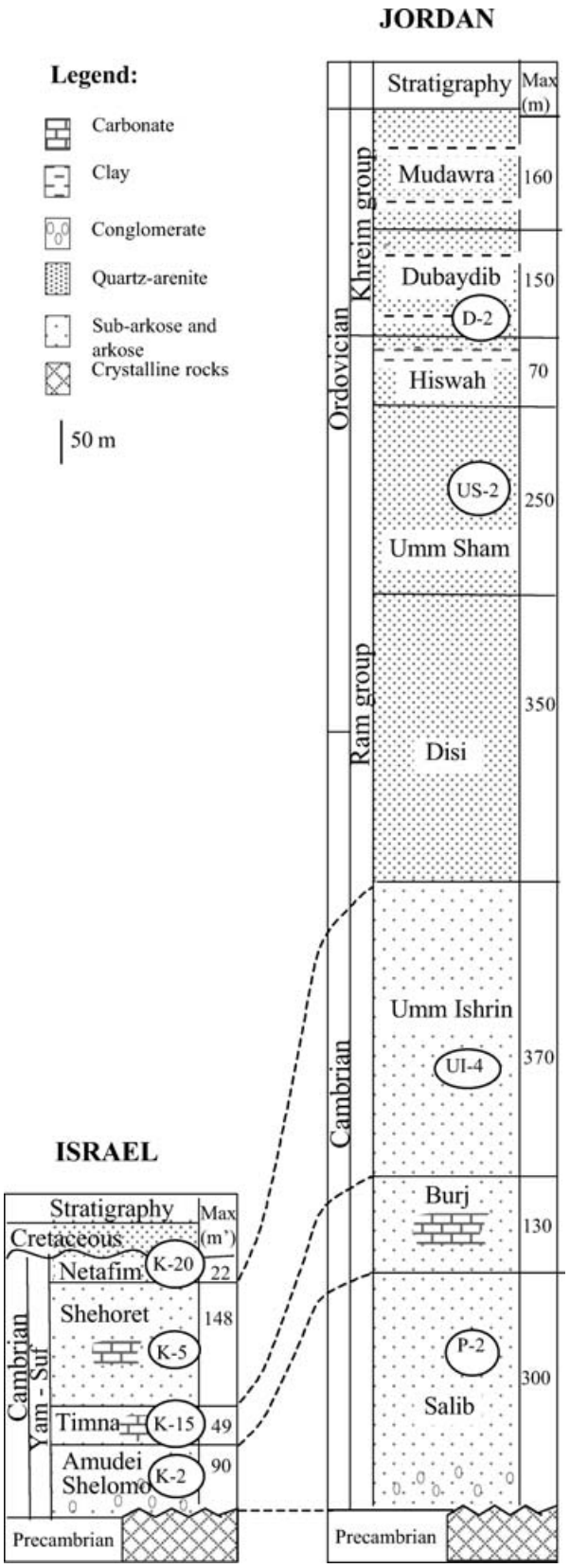

Figure 2. Schematic lithostratigraphic columns of the Cambrian–Ordovician sequence in southern Jordan and the Cambrian section in southern Israel. The Cambrian sections in both countries are similar, although there are significant differences in thickness. Samples studied in the present work are numbered and marked in ellipses.

three sandstone units: the Hiswah Formation, Dubaydib Formation and the lower part of the Mudawwara Formation that also contains glacial deposits (Powell, 1989; Powell, Moh'd & Masri, 1994).

3. Sampling

Zircons were separated from four sandstone samples at different stratigraphic levels from the Cambrian of southern Israel in the Elat area (Timna and Shehoret valleys) and from four samples of Cambrian–Ordovician sandstones of southern Jordan in the El-Quweira area. Sample locations are shown in Figure 1 and their stratigraphic positions and a correlation between the Jordan and Israel stratigraphic levels are presented in Figure 2a and b.

3.a. Samples from southern Israel

Sample K-2 is a subarkose from the Amudei Shelomo Formation that immediately overlies the crystalline basement. It is moderately sorted, and most grains are sub-rounded to sub-angular. Sample K-15 is a coarse-grained, moderately sorted subarkose with sub-rounded grains, from the lower part of the Timna Formation. K-5 is a fine-grained, moderately sorted, subarkose from the Shehoret Formation, and K-20 is a mature quartz arenite from the Netafim Formation that caps the Cambrian section.

3.b. Samples from southern Jordan

The Cambrian–Ordovician section in southern Jordan was sampled in the El Quweira area (Fig. 1). Sample P-2 is coarse-grained arkosic sandstone from the late early Cambrian Salib Formation. It is moderately sorted and most grains have sub-rounded to sub-angular shapes. Sample UI-4 from the Umm-Ishrin Formation is Middle to Upper Cambrian medium-grained quartz-arenite, comparable to the Shehoret Formation. It is well sorted and most of the grains have sub-rounded edges. Sample US-2 from the Early Ordovician Umm Sahm Formation is characterized by coarse-grained, thick-bedded quartz-arenite. It is well sorted and most of the grains have sub-rounded to sub-angular edges. Sample D-2 from the Middle Ordovician Dubaydib Formation is fine-grained, well-sorted sandstone rich in micas.

4. Analytical techniques

Zircons separated from 5–10 kg sandstone samples were prepared by standard techniques. Representative zircon fractions of each sample, usually from the 64 to 150 micron fraction, were mounted in epoxy, polished, coated with gold and scanned by cathodoluminescence imaging (CL). In each sample around 60 grains were dated. This number of grains ensures that there is 95 % confidence that no fraction $f_{act} \geq 0.085$ was missed (Vermeesch, 2004).

U–Th–Pb analyses were made on the Stanford-USGS SHRIMP RG (Reverse Geometry) using the SL13 zircon standard as a reference. Each spot analysis is the average of five scans through nine mass-stations. Ion count rates per mass channel were determined at the time mid-point by linear regression, and data processing and plotting were performed using Isoplot (Ludwig, 1994). Common lead was estimated using the method of Stacey & Kramers (1975) and was generally low. Analytical spots, ~ 30 μm in diameter, were sputtered using a ~ 10 nA O_{2-} primary beam. The primary beam was rastered across the analytical spot for 90 seconds before the analysis to reduce common Pb, and the resulting analyses showed that ^{204}Pb is generally < 0.01 % of the total Pb. Isotope ratios were calibrated against AS57 with an assumed age of 1099 Ma (Paces & Miller, 1993). Zoned grains with wide rims (> 30 μm) were measured in two spots, core and rim. Discordant detrital zircon ages can be difficult to interpret because each grain may have been derived from a different source that might be affected by different Pb loss events (Ross & Parrish, 1991). We set an arbitrary criterion of 10 % Pb loss as the boundary between concordant and discordant results. The ages given as nearly concordant are based on the weighted mean of the $^{207}Pb/^{206}Pb$ and $^{206}Pb/^{238}U$ ages of each grain. For discordant zircons with MSWD (Mean Square of Weighted Deviation) > 10, the $^{206}Pb/^{238}U$ age was used when it was less than 800 Ma, whereas the $^{207}Pb/^{206}Pb$ age was used for zircons with $^{206}Pb/^{238}U$ ages older than 800 Ma, and these were always assumed to be minimum crystallization ages.

5. Results

U–Pb ages from 480 grains from eight samples from Israel and Jordan were measured, and the analytical results are presented in Appendices 1 and 2. Concordia diagrams of all ages obtained in each section are presented in Figure 3a and b, showing that most of the grains have Neoproterozoic ages and that most of the older ages are discordant. In both the Cambrian section of Israel and the Cambrian–Ordovician sections of Jordan, the relative proportion of the concordant grains varies with stratigraphic position (Fig. 3c).

The data obtained for each of the analysed samples are presented as the range of weighted mean ages in Figure 4.

5.a. Ages from the Cambrian of Israel

The four Cambrian sandstone samples from Israel yielded concordant $^{206}Pb/^{238}U$ ages, mainly between 530 and 900 Ma (Figs 3, 4), leading to the conclusion that their major source is a Neoproterozoic basement. The analyses also revealed three older zircon age groups

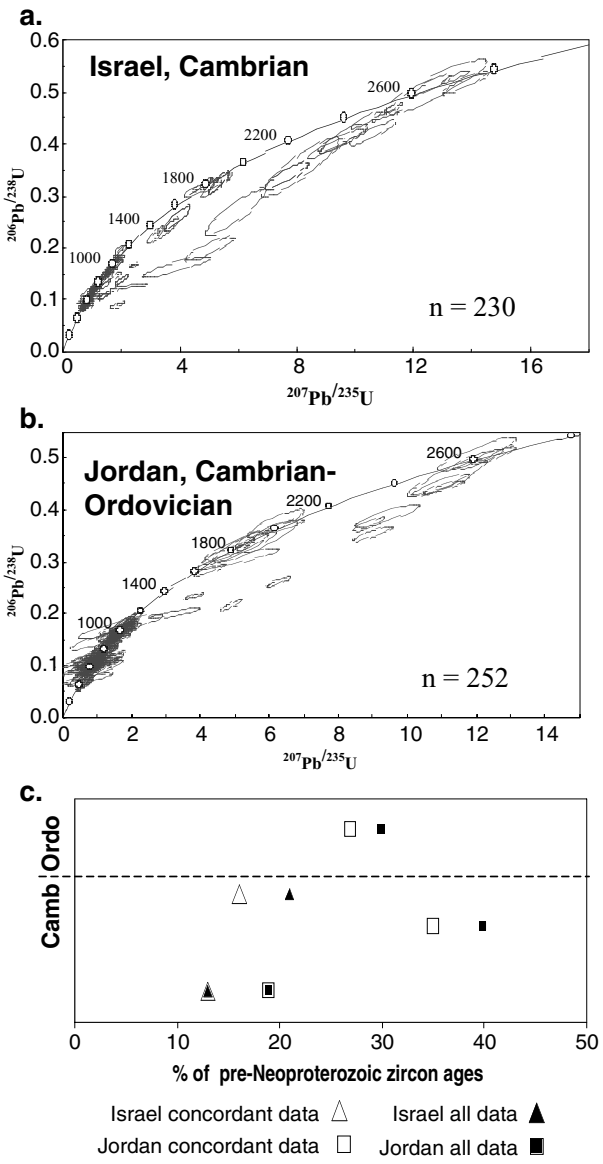

Figure 3. Concordia diagrams of all zircon grains from the Cambrian section in Israel (a), and from the Cambrian–Ordovician section of Jordan (b). Each diagram includes data from four samples, from bottom to top of the successions. Ellipses represent 95 % confidence limits for single-grain analyses. (c) Percentage of pre-Neoproterozoic concordant and disconcordant grains in different stratigraphic levels, through Cambrian–Ordovician time.

(late Archaean to early Neoproterozoic): 0.95–1.10, 1.80–1.90 and 2.60–2.70 Ga (Fig. 4), which appear in all stratigraphic levels.

Sample K-2 from the Amudei Shelomo Formation (the basal unit) yielded 80 % concordant zircon ages, 87 % of which are Neoproterozoic (~ 530–900 Ma). K-2 also contains concordant late Archaean to early Neoproterozoic grains (0.95–1.10 Ga, 1.75–1.85 Ga and 2.65–2.70 Ga).

Upward in the section, in the Timna Formation, the fraction of concordant ages, as well as the proportion of Neoproterozoic Pan-African age zircons, decreases slightly. Sample K-15 produced a 78 % concordance rate, from which 80 % of the ages fall within the Neoproterozoic age interval. About 11 % of the concordant ages lie in the 0.95–1.10 Ga interval and only a few grains yielded 1.7–1.8 Ga and 2.6–2.7 Ga.

Similar age clusters appear in the middle to upper Cambrian Shehoret and Netafim formations but the relative proportions, as well as the proportion of concordant and discordant grains, differ significantly. In the Shehoret Formation, concordant grains make up about 69 % of the population, of which 84 % show Neoproterozoic Pan-African ages. Among the older grains, the 0.95–1.10 Ga group dominates, forming ~ 12 % of the concordant population. The same distribution holds for the supermature quartz arenite of the Netafim Formation. The discordant ages from the Shehoret and Netafim formations (Fig. 4) seem to define two elongated clusters, each of which can be roughly matched with a discordia line whose upper intercepts lie at 1.8–1.9 Ga and 2.6 Ga, respectively. The presence of concordant grains of similar age supports the reliability of these upper intercept ages and suggests that these discordant grains were derived from Early Proterozoic (1.8 Ga) and Late Archaean (2.6 Ga) terranes that were affected by lead loss during the Neoproterozoic.

Although Neoproterozoic detrital zircons dominate the age spectra of the entire Cambrian sandstone in Israel, the percentage of pre-Neoproterozoic ages increases in the upper part of the section and becomes significant (Fig. 3c). The second largest group is the pre-Neoproterozoic 0.95–1.10 Ga that appears in all samples and makes up 5–13 % of the population.

5.b. Ages from the Cambrian and Ordovician of Jordan

The four sandstone samples from Jordan yielded concordant $^{206}Pb/^{238}U$ ages, mainly between 530 and 900 Ma (Figs 3, 4). The analyses also revealed three old zircon age groups (late Archaean to early Neoproterozoic): 0.95–1.10, 1.80–1.90 and 2.60–2.70 Ga (Fig. 4), which appear in all stratigraphic levels.

As in Israel, a gradual up-section decrease in the proportion of Neoproterozoic zircons is observed (Fig. 3c) from 81 % in the Cambrian Salib Formation to 60 % in the overlying Cambrian Umm-Ishrin Formation. In general, the proportion of Neoproterozoic zircon grains in the Cambrian Salib Formation in Jordan is lower than that in its Israeli stratigraphic equivalent (Amudei Shelomo Formation). At the top of the section studied by us, at the middle Ordovician of Jordan, the pre-Neoproterozoic zircons slightly decrease to about 30 % of the entire population.

The pre-Neoproterozoic age clusters detected in Jordan resemble the main clusters in Israel but the relative proportions are different (Fig. 4). In the Salib Formation the pre-Neoproterozoic ages are confined

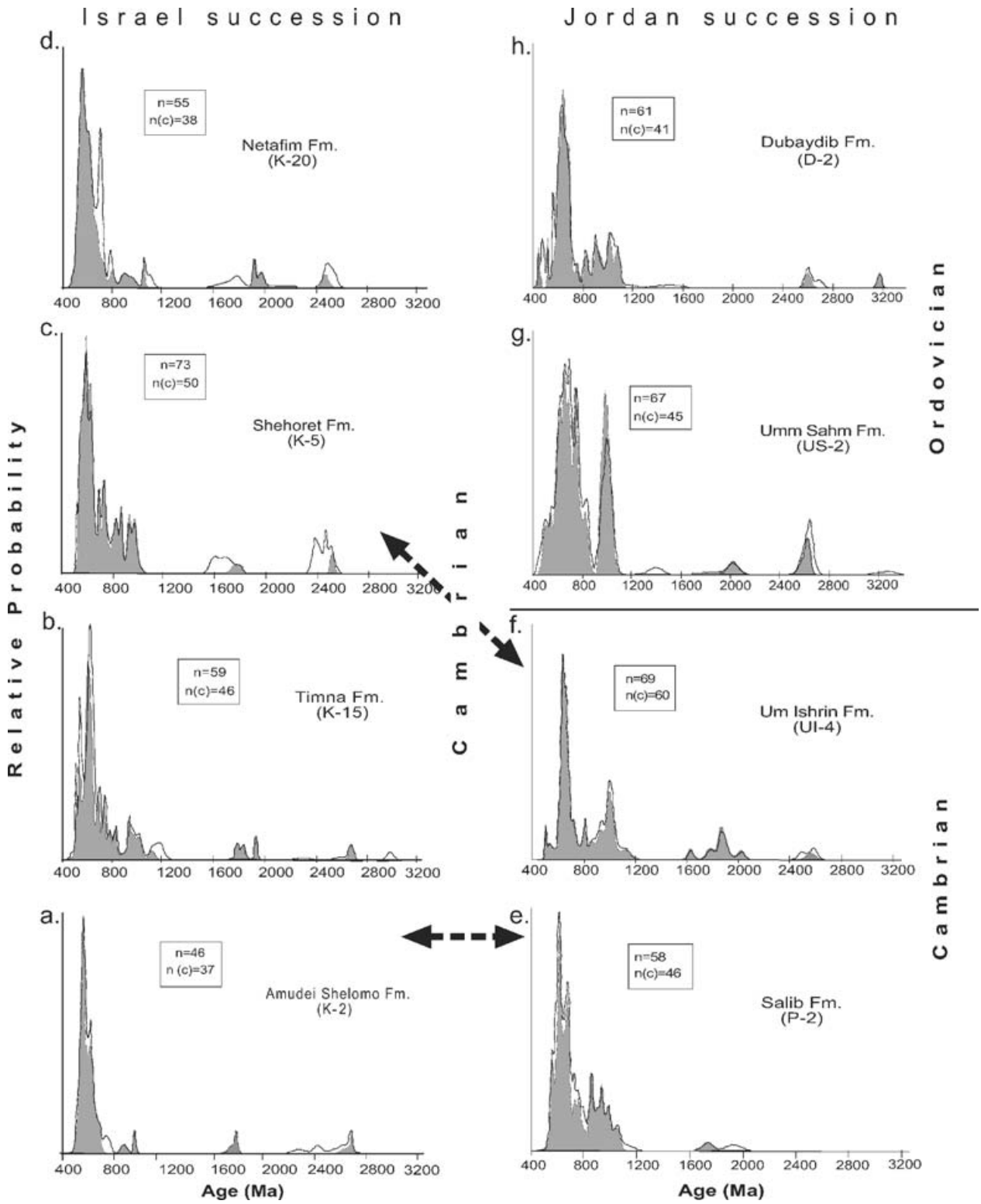

Figure 4. Relative probability histograms of the U–Pb SHRIMP ages of detrital zircons from the Cambrian section of southern Israel and from the Cambrian–Ordovician section in Jordan. The data from the Israel section are from four samples: (a) Amudei Shelomo Formation (K-2), (b) Timna Formation (K-15), (c) Shehoret Formation (K-5) and (d) Netafim Formation (K-20). The Jordanian Cambrian samples are from (e) the Salib Formation (P-2) and (f) the Um-Ishrin Formation (UI-4), and those of Ordovician age are from (g) the Umm-Sahm Formation (US-2) and (h) the Dubaydib Formation (D-2) of the section. The relative probabilities of weighted mean ages of all data are limited by the black curves, whereas the concordant ages histograms are grey-filled. The arrows point to the correlative formations from Israel and Jordan.

to 0.95–1.10 Ga zircons (17 % of the population), whereas in the overlying Umm-Ishrin Formation, 20 % of the zircons fall at 0.95–1.1 Ga and 13 % lie in the 1.65–2.00 Ga range. In the Ordovician section, 0.95–1.1 Ga zircons dominate the pre-Neoproterozoic age spectrum. In the Umm–Sahm Formation, 27 % of the concordant zircons yield ages of 0.95–1.1 Ga and only several grains yield 1.8–1.9 Ga and 2.55–2.65 Ga ages. In the Dubaydib Formation, 22 % of the ages are between 0.95–1.1 Ga and a few grains yielded ~2.6 Ga and ~3.15 Ga. The Dubydib Formation also contains post-Neoproterozoic, pre-Ordovician zircons whose ages fall within the 530–490 Ma range.

To describe better the potential source areas, expanded relative probability diagrams of the age spectra between 0.5–1.2 Ga (Fig. 5) show that more than 60 % of the ages are contained in two groups at 550–580 Ma and 620–640 Ma, although various amounts of 715–720 Ma and 820 Ma age zircons are detected in all samples.

5.c. Detrital zircons younger than the host sediments

Most of the Neoproterozoic zircons contain 50–700 ppm U and concentrations greater than 500 ppm are rare. Most of the 1–1.1 Ga, 1.8–1.9 Ga, and 2.65–2.7 Ga zircons contain 50–400, 50–500 and 200–300 ppm U, respectively (Fig. 6). A negative correlation between age and U concentration appears in relatively young (Late Neoproterozoic) zircons with high U contents (< 500 Ma, > 800 ppm, Fig. 6), indicating that a fast pathway for Pb diffusion had been created due to radiation damage.

These zircons, with concordant U–Pb ages younger than sedimentation ages, were excluded from the relative frequency diagrams presented in Figures 4 and 5. They comprise a few percent of the total population analyzed, appear in each of the eight samples we studied and yielded variable ages between 150 and 440 Ma. These grains have a morphology and internal structure otherwise similar to the 'normal' zircons described above. However, these anomalously young grains are distinguished by having elevated U content (Fig. 6) and Th/U ratio. Thus, we consider that rather than reflecting crystallization, these anomalously young $^{206}Pb/^{238}U$ ages resulted from complete loss of radiogenic Pb enhanced by radiation damage.

6. Zircon structure and morphology

The external and internal morphology of zircon grains can be revealed by visible and CL imaging. These techniques can yield additional information about relative transport distances and on the petrology of the source (igneous or metamorphic). Zircon grains from each of the four age groups (0.5–0.9, 1–1.1, 1.8–1.9, 2.6–2.65 Ga) were examined. Their representative morphologies and CL zoning patterns are shown in Figure 7.

Three types of zircon morphology were observed among the 0.5–0.9 Ga Neoproterozoic grains. (1) Idiomorphic or slightly rounded, typically displaying oscillatory euhedral concentric CL zoning. These zircons were probably derived from an igneous source (Vavra, 1990; Rubatto & Gebauer, 2000). (2) Sub-rounded grains, sometimes with coarse zoning or narrowly banded zones. These zircons were also derived from an igneous source but may have been transported from a more distal source. (3) Rounded zircons, weakly zoned, homogeneous or patchy, that were derived from a metamorphic source (Vavra, 1990; Rubatto & Gebauer, 2000).

In the Cambrian of southern Israel, as well as in the Jordanian succession, the majority of the Neoproterozoic zircons are of Type 1 but there are also a few Type 2 grains. In the upper part of the Israeli section (Shehoret and Netafim formations; Fig. 7), a few rounded Type 3 grains as well as zircon fragments occur.

There is no significant difference in morphology and texture between the pre-Neoproterozoic zircon grains and those of the Neoproterozoic age. The 0.95–1.15 Ga zircons are sub-rounded or rounded, partly with coarse zoning or narrowly banded zones. They were probably also derived from an igneous source. The 1.8–1.9 and 2.6–2.7 Ga grains, either fragments or whole grains, have variable morphology and may have been derived from igneous and/or metamorphic sources such as the East Saharan Craton (Harms, Schandelmeier & Darbyshire, 1990; Stern *et al.* 1994 and references therein) or Oweinat in the southwest desert of Egypt (Klerkx, 1980). These putative source terranes are approximately 1000 km away (Fig. 8).

The Cambrian sandstone from Jordan contains Neoproterozoic age zircons that contain both Type 1 idiomorphic grains and sub-rounded Type 2 grains. The Ordovician sandstone contains mostly idiomorphic and sub-rounded Neoproterozoic age zircon grains, but a few rounded grains also occur (Type 3).

7. Provenance of the Cambrian–Ordovician succession

A comparison of the detrital zircon ages from Israel and Jordan shows many similarities, indicating that on a regional scale these two areas were fed from similar sources. In both sections, most grains are Neoproterozoic, the proportion of pre-Neoproterozoic zircon ages increases up-section, and the pre-Neoproterozoic ages define similar groups. The major difference is in the relative proportions.

The basement immediately underlying the early Palaeozoic cover strata of southern Israel and Jordan, is the juvenile Arabian–Nubian Shield that was formed during the Neoproterozoic (900–530 Ma) Pan-African Orogeny, and is exposed in Egypt, Sudan, Saudi Arabia, Yemen, Somalia, Ethiopia, Eritrea, Jordan and Israel

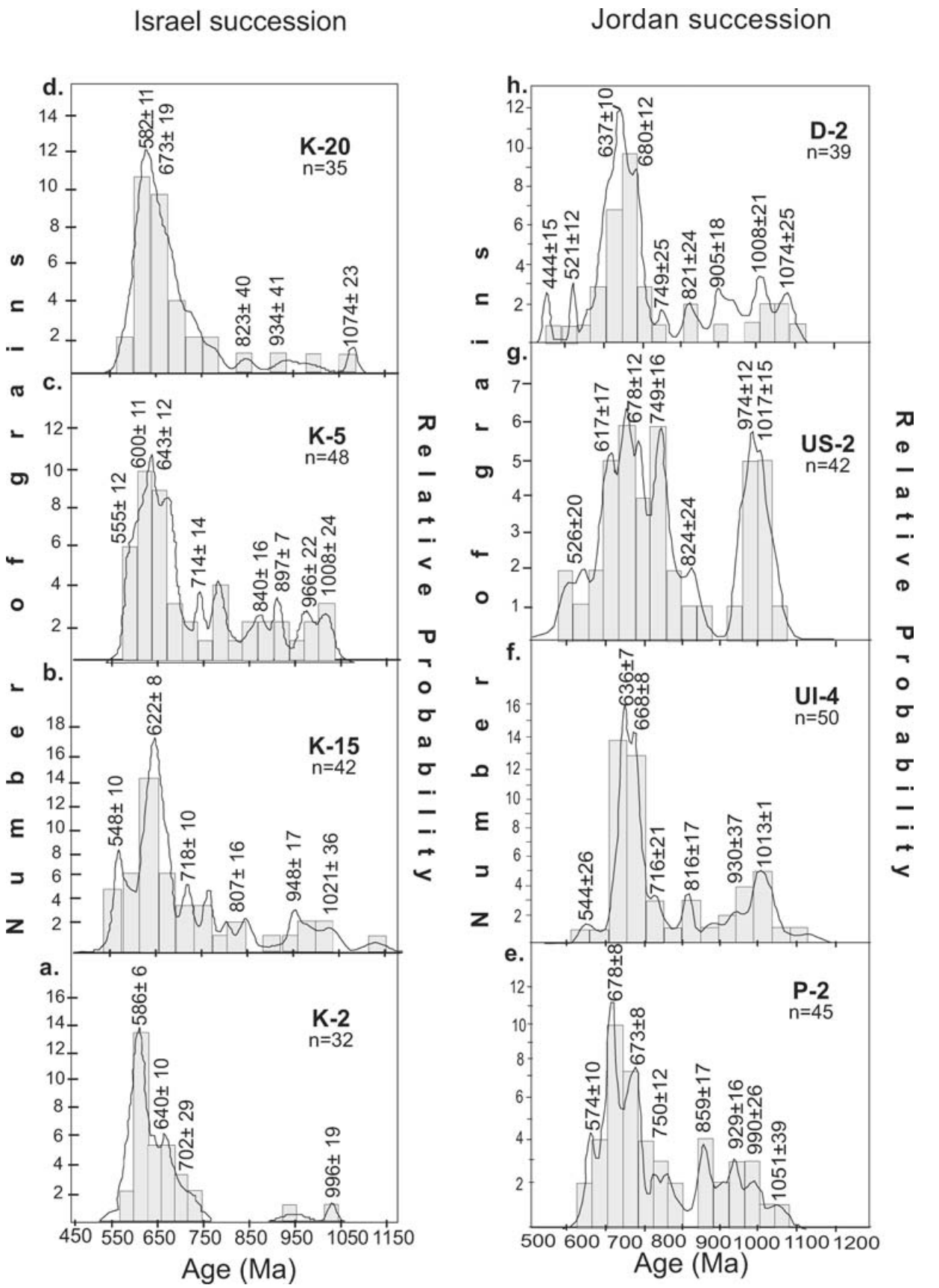

Figure 5. Expanded relative probability histograms for concordant zircon ages younger than 1.2 Ga from the Cambrian section of Israel and from the Cambrian–Ordovician section in Jordan. The superimposed bar graphs indicate the results of mixture modelling, namely each age subgroup with its 95 % confidence limits and relative abundance.

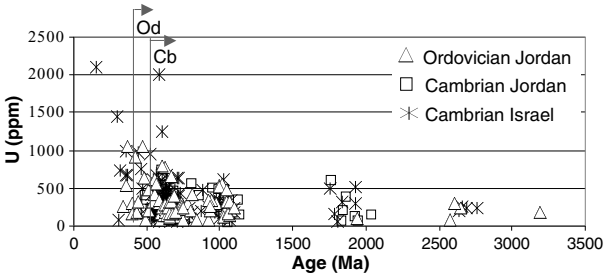

Figure 6. U concentrations versus concordant ages of zircon grains. Results of ~480 zircon grains from Israel and Jordan are plotted. Cb – Cambrian period; Od – Ordovician period.

(Fig. 1; Bentor, 1985; Stein & Goldstein, 1996; Stern, 2002; Kröner, 1984; Kröner *et al.* 1987; Stern *et al.* 1994; Petters, 1991 and references therein).

The lowest Cambrian units in Israel (Amudei Shelomo) and Jordan (Salib) are dominated by subarkose or arkose and contain a basal conglomerate deposited on rough topography. They both appear to have been derived from a proximal source, and their detrital zircon age histogram is taken to describe the composition of the Arabian–Nubian Shield at or near the source. Within the Neoproterozoic interval, detrital zircons yielding 550–670 Ma ages predominate in all stratigraphic levels. The most likely source of detrital zircons of this age in the Cambrian–Ordovician section is the widespread late proterozoic calk-alkaline and alkaline granites which are ubiquitous in the Arabian–Nubian Shield and form more than 50 % of its exposed rock (Bentor, 1985; Eyal, Eyal & Kröner, 1991; Stern, 1994).

Various amounts of 715–720 Ma and 820 Ma age zircons are detected in all Cambrian samples. Metavolcanic rocks, schists and granites of this age are common in the Arabian–Nubian Shield (e.g. Dixon, 1981; Kröner, Eyal & Eyal, 1990; Stern & Kröner, 1993; Fleck *et al.* 1980; Stoeser, 1986). In addition, detrital zircons from the Neoproterozoic Elat Schist, in the immediate vicinity of the Cambrian sandstone exposures, yielded U–Pb ages of 820 Ma (our unpub. data).

The presence of early Neoproterozoic and older age zircons suggests that a minor exposure of an older crust existed within the otherwise Neoproterozoic Arabian–Nubian Shield in the proximity of Elat and southern Jordan. Stacey & Stoeser (1983) inferred older continental basement in the eastern Arabian shield from common Pb analyses. Evidences for an older crust were provided also by Nd isotopes from Yemen, Somalia and Eastern Ethiopia (Stern, 2002). Dixon (1981) and Wust, Todt & Kröner (1987) showed that the western part of the Arabian–Nubian Shield locally contains detritus derived from pre-Neoproterozoic sources that was incorporated into the Arabian–Nubian Shield during Neoproterozoic times.

This study demonstrates a general up-section increase in the fraction of detrital zircons displaying pre-Neoproterozoic ages, indicating a progressive change of provenance with time and an increase in material derived from more distal sources. When deposition of the Palaeozoic succession began, the main sources of the Amudei Shelomo Formation in southern Israel were late Neoproterozoic rocks of the Arabian–Nubian Shield. Potential source rocks are ubiquitous in the crystalline basement underlying the study area and are exposed in Sinai south of Elat. As the transgression continued, early Palaeozoic sediments covered the proximal source areas such that detritus for the overlying sedimentary unit had to be supplied from a source further to the south. While still dominated by late Neoproterozoic rocks, the more distal source area(s) contained a larger proportion of pre-Neoproterozoic rocks, which are more common on the periphery of the Arabian–Nubian Shield. Examples include the Afif Terrane (Stacey & Hedge, 1984) or Oweinat area, at a distance of about 1000 km from Elat (Klerx, 1980; Sultan *et al.* 1990; Fig. 8).

The 0.95–1.1 Ga (Kibaran) age peak in the spectrum is of particular interest. Zircons of this age are subrounded, some with coarse zoning. The nearest Kibaran age crystalline outcrop is now about 3000 km south of our study areas (Kröner, 2001; Fig. 8), but the shape of the Kibaran age grains are inconsistent with long distance transport. Moreover, we note that the lowermost rock units such as the Amudei Shelomo in Israel and particularly the Salib Formation in Jordan (1) are dominated by subarkose, (2) contain a basal conglomerate, (3) seem not to have been derived from a distal source, and (4) contain Kibaran age detrital zircons. To explain the Kibaran zircons from the Cambrian succession of Elat, Avigad *et al.* (2003) suggested that Kibaran material was transported from East Africa towards the margins of Gondwana by Neoproterozoic glaciers, and that the glacial detritus was later reworked into the lower Palaeozoic section by the Cambrian–Ordovician fluvial system. This interpretation implies that glacial tillite and/or diamictites were deposited in the Arabian–Nubian Shield in the vicinity of Elat and south Jordan. Neoproterozoic diamictite successions, considered to be products of the 720–750 Ma Sturtian glaciation, have been reported from the southern part of the Arabian–Nubian Shield in Ethiopia (the Negash diamictite) and Eritrea (Miller *et al.* 2003; Beyth *et al.* 2003). These diamictites contain Kibaran age zircons (D. Avigad, unpub. data). Dixon (1981) reported a 30 cm boulder yielding a 1.1 Ga U–Pb zircon age (an upper intercept) from a succession described as a meta-conglomerate in the Eastern Desert of Egypt, but a provenance does not exist in the vicinity of the outcrop and we suspect it may represent glacial transport.

In Jordan the 0.95–1.1 Ga group makes up 17–27 % of the concordant grains, whereas in Israel it makes

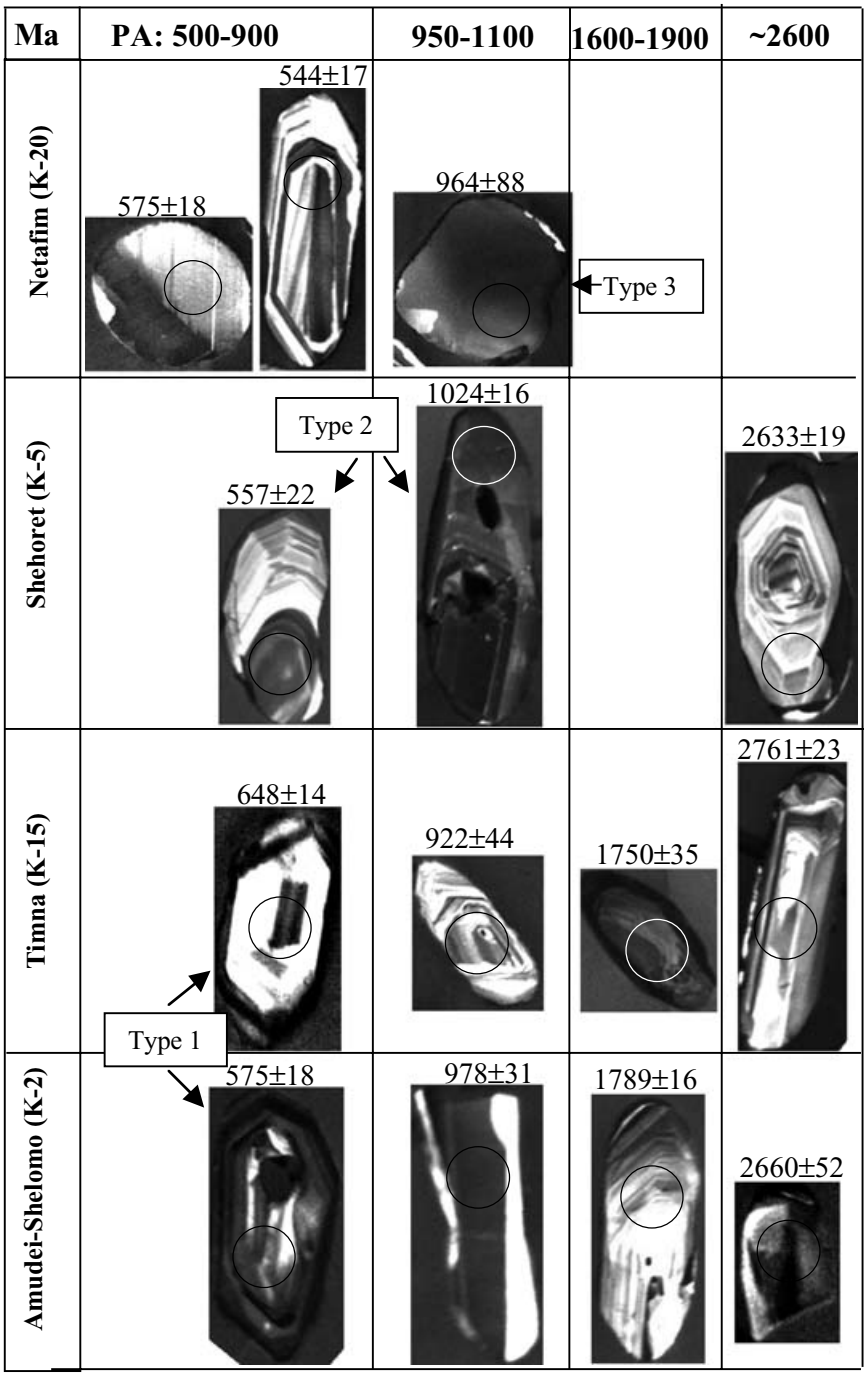

Figure 7. Representative scanning electron microscope cathodoluminiscence (CL) images of sectioned zircon grains from the Cambrian siliciclastic section of Israel. The internal and external shapes of zircon grains from each unit were examined with respect to the different age groups (0.5–0.9, 0.95–1.1, 1.6–1.9, ~ 2.6 Ga.). Locations of spot analyses and ages (Ma) are marked. At the base of the section, Pan-African grains are mostly idiomorphic or slightly rounded, typically displaying oscillatory euhedral concentric CL zoning (types 1 and 2, see text). At the upper part of the section rounded and weakly zoned zircons (type 3) also appear. The pre-Pan-African zircons display wider morphological variations.

up only 5–13 % of the concordant grains. Prior to the Neogene northward drift of Arabia (Freund *et al.* 1970), the Jordanian section was located ~ 100 km south of Elat. Since the Jordanian section was located further to the south than its Israeli counterpart at the time of deposition of the sandstone, and since the transport was generally from south to north, the Jordanian section was closer to any putative Kibaran age sources. If any movement in the range of 100 km makes a difference, Kibaran rocks (possibly as pebbles in a diamictite) resided at a distance of several hundreds of kilometres south of the study area, since distal Kibaran source rocks would not make a difference between Israel and Jordan successions. The ubiquitous presence of

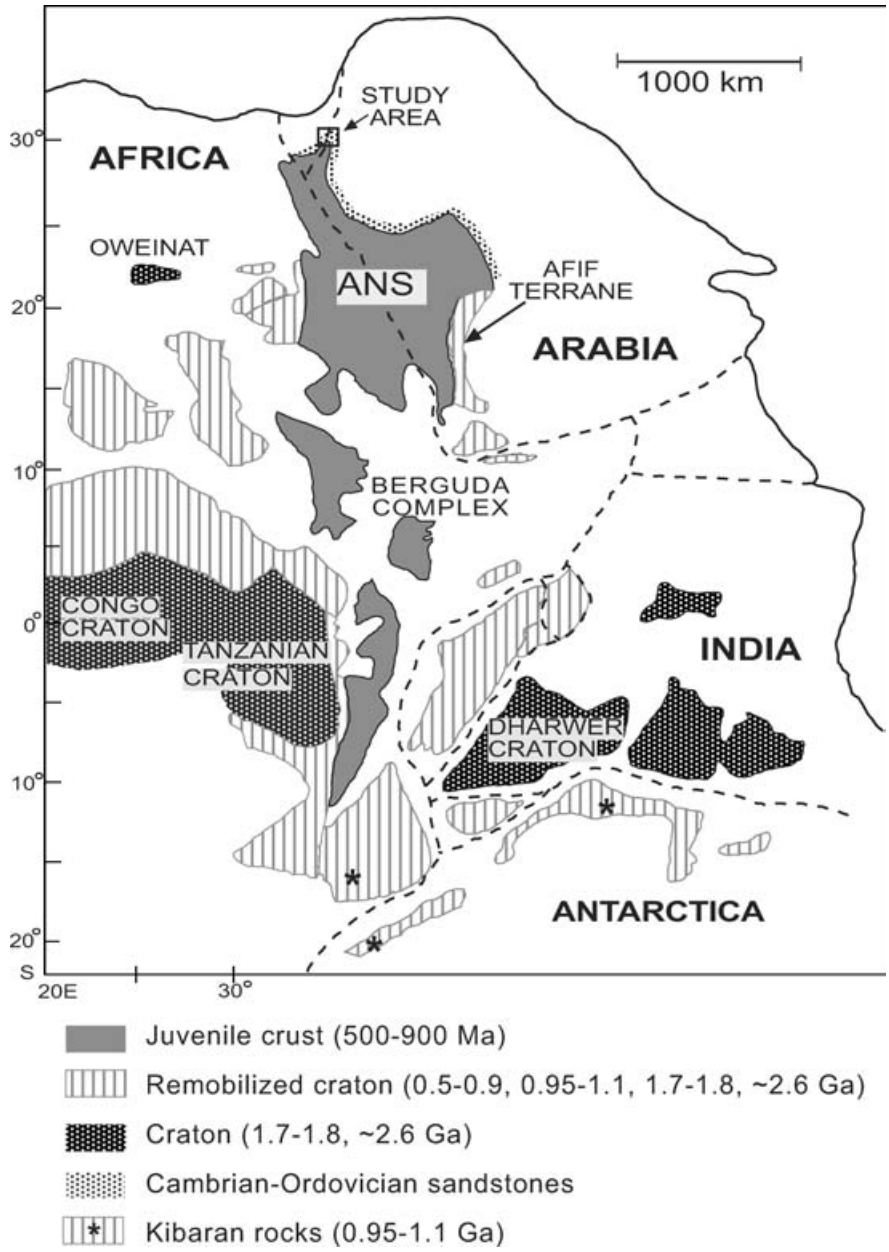

Figure 8. Illustration of Gondwana palaeogeography at the beginning of Palaeozoic times, showing major geological constituents in Africa and Arabia. Juvenile crust represents rocks with U–Pb ages of 500–900 Ma (e.g. Eyal, Eyal & Kröner, 1991; Beyth *et al.* 1994; Ayalew *et al.* 1990). Remobilized areas contain 1.7–1.8 Ga and ~2.6 Ga rocks remobilized during Neoproterozoic times (500–900 Ma) (e.g. Klerkx, 1980; Sultan *et al.* 1990, 1994; Kröner, 2001 and references therein; Stacey & Hedge, 1984). Asterisks mark places where 0.95–1.1 Ga rocks are exposed. Old craton rocks, mainly in the south, are composed of rocks yielding U–Pb ages of 1.7–1.8 and ~2.6 Ga (e.g Klerkx, 1980; Kröner, 2001 and references therein). Modified after Stern (1994) and Kröner (2001).

0.9–1.1 Ga detrital zircons may, alternatively, indicate that crust of this age exists in the Arabian–Nubian Shield, although this has not been found.

The source(s) of other pre-Neoproterozoic age zircons found in the succession could be crustal exposures such as the northern part of the Congo-Tanzanian, the Dhrawer cratons (Kröner, 2001), or the Gebel Uweinat area, where pyroxene granulites have yielded a whole-rock Rb–Sr age of ~2.65 Ga and ~1.85 Ga (Klerkx, 1980, recalculated by Cahen *et al.* 1984). U–Pb zircon ages of the Western Desert of Egypt, east of the Gebel Uweinat area and west of the Eastern Desert, yielded a crystallization age of > 2.67 Ga and metamorphic age of 2.0 Ga (Sultan *et al.* 1994). Those exposures can be a plausible provenance for the ~1.7–1.8 Ga and ~2.6–2.7 Ga zircons (Fig. 8).

The Ordovician section in Jordan also contains 530–440 Ma post-Neoproterozoic grains, implying their possible derivation from sources such as the peralkaline granites of Ras Gharib in the eastern desert of Egypt (Abdel-Rahaman & Doig, 1987) or intrusions in the

Red Sea Hills of Sudan (Hohndorf, Meinhold & Vail, 1994) where Cambrian–Ordovician igneous activity occurred.

8. Conclusions

Our results show that when deposition of the Cambrian sandstone began, the cover successions of northeast Africa and Arabia were mainly sourced by late Neoproterozoic Pan-African rocks of the northern Arabian–Nubian shield. As deposition spread southward, the proximal crystalline source rocks were covered such that detritus for the younger sedimentary units was increasingly supplied by a distal source further to the south. While still dominated by Neoproterozoic Pan-African basement, the more distal source contained a larger proportion of older rocks. We interpret the detrital zircon age spectrum of these early Palaeozoic strata as representing the progressive southward migration of the source area and the simultaneous progressive blanketing of northeast Africa and Arabia by Cambrian and Ordovician cover strata. Our data is not inconsistent with the entire Arabian–Nubian Shield being covered by a thin sandstone veneer by late Ordovician times (e.g. Schmidt, Hadley & Stoeser, 1979).

Acknowledgements. Our study was funded by the Israel Ministry of Energy and Infrastructure. We thank Z. Garfunkel, M. Beyth, N. Porat and Y. Katzir for advice and discussions and O. Navon for providing access to his Raman laboratory. Comments by R. J. Stern, P. Meyroo and Y. Kolodny and reviews by P. Cawood and Ghaleb Jarrar helped to improve this manuscript and are greatly appreciated.

References

ABDEL-RAHMAN, A. M. & DOIG, R. 1987. The Rb–Sr Geochronological Evolution of the Ras Gharib segment of the Northern Nubian shield. *Journal of the Geological Society, London* **144**, 577–86.

ALSHARHAN, A. S. & NAIRN, A. E. M. 1997. *Sedimentary basins and petroleum geology of the Middle East*. Amsterdam: Elsevier, 811 pp.

AMIREH, B. S. 1991. Mineral composition of the Cambrian–Cretaceous Nubian series of Jordan: provenance, tectonic setting and climatological implications. *Sedimentary Geology* **71**, 99–119.

AVIGAD, D., KOLODNER, K., MCWILLIAMS, M., PERSING, H. & WEISSBROD, T. 2003. Origin of northern Gondwana Cambrian sandstone revealed by detrital zircon SHRIMP dating. *Geology* **31**, 227–30.

AYALEW, T., BELL, K., MOORE, J. M. & PARRISH, R. R. 1990. U–Pb and Rb–Sr geochronology of the Western Ethiopian Shield. *Geological Society of America Bulletin* **102**, 1309–16.

BENDER, F. 1974. *Geology of Jordan: Contribution to the regional geology of the world*. Berlin: Gebrueder Borntraeger, 196 pp.

BENNACEF, A., BEUF, S., BIJU-DUVAL, B., DE CHARPAL, O. & GARIEL, O. 1971. Example of Cratonic sedimentation: Lower Palaeozoic of Algerian Sahara. *American Association of Petroleum Geologists Bulletin* **55**, 2225–45.

BENTOR, Y. K. 1985. The crustal evolution of the Arabo-Nubian massif with special reference to the Sinai peninsula. *Precambrian Resarch* **28**, 1–74.

BENTOR, Y. K., VROMAN, A. & ZAK, I. 1987. *Geological Map of Israel: southern sheet*. 1:250000. Geological Survey of Israel.

BEYTH, M., AVIGAD, D., WETZEL, H. U., MATTHEWS, A. & BERHE, S. M. 2003. Crustal exhumation and indications for Snowball Earth in the East African Orogen: north Ethiopia and east Eritrea. *Precambrian Research* **123**, 187–201.

BEYTH, M., STERN, R. J., ALTHERR, R. & KRÖNER, A. 1994. The late Precambrian Timna igneous complex, southern Israel. Evidence for comagmatic-type sanukitoid monzodiorite and alkali granite magma. *Lithos* **31**, 103–24.

BURKE, K. & KRAUS, J. U. 2000. Deposition of immense Cambro-Ordovician sandstone bodies, now exposed mainly in N. Africa and Arabia, during the aftermath of the final assembly of Gondwana. *Geological Society of America, Abstracts with Programs* **32**(7), 249.

BURKE, K. & MACGREGOR, D. & CAMERON, N. 2003. Africa's Petroleum systems: four tectonic Aces in the past 600 million years. In *Petroleum geology of Africa: new themes and developing technologies* (eds T. J. Arthur, D. S. MacGregor and N. Cameron), pp. 21–60. Geological Society of London, Special Publication no. 207.

CAHEN, L., SNELLING, N. J., DELHAL, T. & VAIL, J. R. 1984. *The geochronology and evolution of Africa*. London: Oxford Science, 496 pp.

DIXON, T. H. 1981. Age and chemical characteristics of some pre-Pan-African rocks in the Egyptian shield. *Precambrian Research* **14**, 119–33.

EYAL, Y., EYAL, M. & KRÖNER, A. 1991. Geochronology of the Elat terrain, metamorphic basement, and its implication for crustal evolution of the NE part of the Arabian–Nubian shield. *Israel Journal of Earth Sciences* **40**, 5–16.

FLECK, R. J., GREENWOOD, W. R., HADELY, D. G., ANDERSON, R. E. & SCHMIDT, D. L. 1980. *Rubidium–strontium geochronology and plate-tectonic evolution of the southern part of the Arabian Shield*. U. S. Geological Survey Professional Paper no. 1131.

FREUND, R., GARFUNKEL, Z., ZAK, I., GOLDBERG, M., WEISSBROD, T. & DERIN, B. 1970. Shear along Dead Sea Rift. *Philosophical Transactions of the Royal Society of London, Series A: Mathematical and Physical Sciences* **267**, 107–27.

GARFUNKEL, Z. 1978. The Negev: Regional synthesis of sedimentary basins. *International Congress of Sedimentology, 10th, Jerusalem, Guidebook* **1**, 33–110.

GARFUNKEL, Z. 1999. History and paleogeography during the Pan-African orogen to stable platform transition: reappraisal of the evidence from Elat area and the northern Arabian–Nubian Shield. *Israel Journal of Earth Sciences* **48**, 135–57.

GARFUNKEL, Z. 2002. Early Palaeozoic sediments of NE Africa and Arabia: Products of continental-scale erosion, sediment transport, and deposition. *Israel Journal of Earth Sciences* **51**, 135–56.

GAUDETTE, H. E. & HURLEY, P. M. 1979. Where were the Pan-African mountains? No evidence of 500 My detrital zircons. *Tectonophysics* **54**, 211–30.

HARMS, U., SCHANDELMEIER, H. & DARBYSHIRE, D. P. F. 1990. Pan-African reworked early/middle Proterozoic crust in NE Africa west of the Nile: Sr and Nd isotope evidence. *Journal of the Geological Society, London* **147**, 859–72.

HOHNDORF, A., MEINHOLD, K. D. & VAIL, J. R. 1994. Geochronology of anorogenic igneous complexes in the Sudan – isotopic investigations in north Kordofan, the Nubian Desert and the Red-Sea Hills. *Journal of African Earth Sciences* **19**, 3–15.

JARRAR, G., WACHENDORF, H. & ZELLMER, H. 1991. The Saramuj Conglomerate: evolution of a Pan-African molasse sequence from south-west Jordan. *Neues Jahrbuch für Geologie und Paläontologie, Monatshefte* **6**, 335–56.

JOHNSON, P. R. 2003. Post-amalgamation basins of the NE Arabian shield and implications for Neoproterozoic III tectonism in the northern East African orogen. *Precambrian Research* **123**, 321–37.

KARCZ, J. & KEY, C. A. 1966. Note on the pre-Palaeozoic morphology of the basement in the Timna area (southern Israel). *Israel Journal of Earth Sciences* **15**, 47–56.

KLERKX, J. 1980. Age and metamorphic evolution of the basement complex around Jabal al'Awaynat. *Symposium on the Geology of Libya* **2**, 901–6.

KLITZSCH, E. 1981. Lower Palaeozoic rocks of Lybia, Egypt and Sudan. In *Lower Palaeozoic rocks of the middle east, eastern and southern Africa and Antarctica* (ed. C. H. Holland), pp. 131–63. London: Wiley.

KLITZSCH, E., HARMS, J. C., LEJAL-NICOL, A. & LIST, F. F. 1979. Major subdivisions and depositional environments of Nubia strata, southwestern Egypt. *American Association of Petroleum Geologists Bulletin* **63**, 974–76.

KRÖNER, A. 1984. Late Precambrian plate tectonics and orogeny: a need to redefine the term Pan-African. In *African geology* (eds J. Klerkx and J. Michot), pp. 23–8. Tervuren: Musée R. L'Afrique Centrale.

KRÖNER, A. 2001. The Mozambique belt of East Africa and Madagascar: Significance of zircon and Nd model ages for Rodinia and Gondwana supercontinent formation and dispersal. *South African Journal of Geology* **104**, 151–66.

KRÖNER, A., GREILING, R., REISCHMANN, T., HUSSEIN, I. M., STERN, R. J., DURR, S., KRUGER, J. & ZIMMER, M. 1987. Pan-African crustal evolution in the Nubian segment of north-eastern Africa. In *Proterozoic lithospheric evolution* (ed. A. Kröner), pp. 235–57. American Geophysical Union, Geodynamics Series no. 17.

KRÖNER, A., EYAL, M. & EYAL, Y. 1990. Early Pan-African evolution of the basement around Elat, Israel, and the Sinai Peninsula revealed by single zircon evaporation dating, and implications for crustal accretion rates. *Geology* **18**, 545–8.

LUDWIG, K. R. 1994. *Isoplot, a plotting and regression program for radiogenic isotope data, ver. 2.71*. Revision to U.S. Geological Survey Open-File Report 91-445.

MCKEE, E. D. 1962. Origin of the Nubian and similar sandstones. *Geologische Rundschau* **52**, 551–87.

MILLER, N. R., ALENE, M., SACCHI, R., STERN, R. J., CONTI, A., KRÖNER, A. & ZUPPI, G. 2003. Significance of the Tambien Group (Tigri, N. Ethiopia) for Snowball earth events in the Arabian–Nubian Shield. *Precambrian Research* **121**, 263–83.

PACES, J. B. & MILLER, J. D. 1993. U–Pb ages of the Duluth complex and related mafic intrusions, northeastern Minnesota: geochronologic insights into physical petrogenetic, paleomagnetic and tectonomagnetic processes associated with the 1.1 Ga mid-continent rift system. *Journal of Geophysical Research* **98**, 13997–14013.

PETTERS, S. W. 1991. *Regional Geology of Africa*. Springer-Verlag, 722 pp.

POWELL, J. H. 1989. Stratigraphy and sedimentation of the Phanerozoic rocks in central and south Jordan. Part A: Ram and Khreim Groups. *Natural Resources Authority, Amman, Geological Bulletin* **11**, 62 pp.

POWELL, J. H., MOH'D, B. K. & MASRI, H. 1994. Late Ordovician–Early Silurian glaciofluvial deposits preserved in palaeovalleys in South Jordan. *Sedimentary Geology* **89**, 303–14.

ROSS, G. M. & PARRISH, R. R. 1991. Detrital zircon geochronology of metasedimentary rocks in the southern Omineca Belt, Canadian Cordillera. *Canadian Journal of Earth Sciences* **28**, 1254–70.

RUBATTO, D. & GEBAUER, D. 2000. Use of cathodoluminescence for U–Pb zircon dating by ion microprobe: some examples from high-pressure rocks of the western Alps. In *Cathodoluminescence in geosciences* (eds M. Pagel, V. Barbin, P. Blanc and D. Ohnenstetter), pp. 373–400. Berlin: Springer.

SCHMIDT, D. L., HADLEY, D. G. & STOESER, D. B. 1979. Late Proterozoic crustal history of the Arabian Shield, southern Klajd Province, Kingdom of Saudi Arabia. *Institute of Applied Geology* **2**, 41–58.

SELLEY, R. C. 1972. Diagnosis of marine and non-marine environments from the Cambro-Ordovician sequence of Jordan. *Journal of the Geological Society, London* **128**, 135–50.

SHACKLETON, R. M. 1986. Precambrian collision tectonics in Africa. In *Collision Tectonics* (eds M. P. Coward and A. C. Ries), pp. 329–49. Geological Society of London, Special Publication no. 19.

STACEY, J. S. & HEDGE, C. E. 1984. Geochronologic and isotopic evidence for early Proterozoic crust in the eastern Arabian Shield. *Geology* **12**, 310–13.

STACEY, J. S. & KRAMERS, J. D. 1975 Approximation of terrestrial lead isotope evolution by a two-stage model. *Earth and Planetary Science Letters* **26**, 207–21.

STACEY, J. S. & STOESER, D. B. 1983. Distribution of oceanic and continental leads in the Arabian–Nubian-Shield. *Contributions to Mineralogy and Petrology* **84**, 91–105.

STEIN, M. & GOLDSTEIN, S. L. 1996. From plume head to continental lithosphere in the Arabian–Nubian shield. *Nature* **382**, 773–8.

STERN, R. J. 2002. Crustal evolution in the East African Orogen: a neodymium isotopic perspective. *Journal of African Earth Sciences* **34**, 109–17.

STERN, R. J. 1994. Arc assembly and continental collision in th Neoproterozoic east African orogen – inplications for the consolidation of Gondwanaland. *Annual Review of Earth and Planetary Sciences* **22**, 319–51.

STERN, R. J. & KRÖNER, A. 1993. Late precambrian crustal evolution in NE Sudan – isotopic and geochronological constarints. *Journal of Geology* **101**(5), 555–74.

STERN, R. J., KRÖNER, A., BENDER, R., REISCHMANN, T. & DAWOUD, A. S. 1994. Precambrian Basement around Wadi-Halfa, Sudan – a New Perspective on the Evolution of the East Saharan Craton. *Geologische Rundschau* **83**, 564–77.

STOESER, D. B. 1986. Distribution and tectonic setting of plutonic rocks of the Arabian Shield. *Journal of African Earth Sciences* **4**, 21–46.

SULTAN, M., CHAMBERLAIN, K. R., BOWRING, S. & ARVIDSON, R. E. 1990. Geochronological and isotopic evidence for involvment of pre-Pan-African crust in the Nubian Shield, Egypt. *Geology* **18**, 761–4.

SULTAN, M., TUCKER, R. D., EL-ALFY, Z., ATTIA, R. & RAGAB, A. G. 1994. U–Pb (zircon) ages for the gneissic terrane west of the Nile, southern Egypt. *Geologische Rundschau* **83**, 514–22.

VERMEESCH, P. 2004. How many grains are needed for a provenance study? *Earth and Planetary Science Letters* **224**, 441–51.

VAVRA, G. 1990. On the kinematics of zircon growth and its petrogenetic significance: a cathodoluminescence study. *Contributions to Mineralogy and Petrology* **106**, 90–9.

WEISSBROD, T. 1969. The Palaeozoic of Israel and Adjacent Countries: Part I: The subsurface Palaeozoic stratigraphy of southern Israel. *Israel Geological Survey Bulletin* **47**, 22 pp.

WEISSBROD, T. & NACHMIAS, Y. 1986. Stratigraphic significance of heavy minerals in the Late Precambrian Mesozoic clastic sequence (Nubian Sandstone) in the near East. *Sedimentary Geology* **47**, 263–91.

WILLIS, K. M., STERN, R. J., & CLAUER, N. 1988. Age and geochemistry of Late Precambrian sediments of the Hammamat series from Northeastern Desert of Egypt. *Precambrian Research* **42**, 173–87.

WOLFART, R. 1981. Lower Palaeozoic rocks of the Middle East. In *Lower Palaeozoic rocks of the middle east, eastern and southern Africa and Antarctica* (ed. C. H. Holland), pp. 5–126. London: Wiley.

WUST, H. J., TODT, W. & KRÖNER, A. 1987. Conventional and single grain zircon ages for metasediments and granite clasts from the eastern desert of Egypt: evidence for active continental margin evolution in Pan-African times. *Terra Cognita* **7**, 165.

Appendix 1. U–Pb geochronology data for detrital zircons separated from Cambrian–Ordovician sandstone in southern Jordan

						Radiogenic ratios				Age (Ma)						
Grain. Spot no.	U (ppm)	Th (ppm)	Th/U	Pb* (ppm)	$^{204}Pb/^{206}Pb$	$^{206}Pb/^{238}U$	±	$^{207}Pb/^{235}U$	±	$^{206}Pb/^{238}U$	±	$^{207}Pb/^{206}Pb$	±	W.M.† age	±	% discord
P2-1	358	196	0.55	41	0.00006	0.1090	0.0016	0.9101	0.0422	667	9	623	94	667	9	107
P2-2	568	703	1.24	108	0.00008	0.1527	0.0017	1.6133	0.0465	916	9	1112	51	1112	51	82
P2-3	290	234	0.80	43	0.00052	0.1310	0.0028	1.4159	0.0874	793	16	1157	114	800	16	69
P2-4	167	143	0.85	31	0.00012	0.1637	0.0042	1.5622	0.1087	977	23	905	132	975	23	108
P2-5	132	75	0.57	15	0.00001	0.1096	0.0024	0.9624	0.0505	670	14	732	99	671	14	92
P2-6	1233	380	0.31	65	0.00036	0.0530	0.0006	0.4693	0.0206	333	3	747	90	747	90	45
P2-7	284	74	0.26	28	0.00008	0.1018	0.0024	0.8389	0.0564	625	14	596	135	624	14	105
P2-8	132	127	0.96	15	0.00001	0.1011	0.0017	0.8601	0.0755	621	10	664	191	621	10	94
P2-9	409	261	0.64	45	0.00015	0.1011	0.0019	0.9302	0.0778	621	11	830	175	621	11	75
P2-10	256	431	1.69	36	0.00062	0.1051	0.0049	0.7829	0.0918	644	29	372	247	641	28	173
P2-11	284	128	0.45	33	−0.00015	0.1112	0.0026	0.9800	0.0577	680	15	739	113	681	15	92
P2-12	46	28	0.62	5	−0.00107	0.0933	0.0039	1.0301	0.1484	575	23	1198	287	579	23	48
P2-13.1	222	167	0.75	22	0.00001	0.0910	0.0015	0.7527	0.0538	561	9	604	153	561	9	93
P2-13.2	262	248	0.95	30	0.00001	0.0991	0.0013	0.8103	0.0293	609	8	579	71	609	8	105
P2-15.1	113	63	0.56	15	0.00001	0.1238	0.0025	1.1441	0.0577	753	14	838	94	755	14	90
P2-16	128	108	0.84	14	0.00001	0.1012	0.0046	0.9793	0.1029	621	27	934	195	627	27	67
P2-17	321	165	0.51	37	0.00025	0.1111	0.0021	0.9393	0.0943	679	12	651	221	679	12	104
P2-18	69	56	0.82	9	0.00140	0.1188	0.0050	0.6898	0.4155	724	29	0	0	724	29	0
P2-19	64	20	0.32	7	0.00001	0.1149	0.0035	0.8825	0.0715	701	20	442	167	697	20	159
P2-20	73	29	0.40	7	0.00087	0.0980	0.0036	0.6402	0.1883	602	21	69	878	602	21	869
P2-21	240	25	0.10	23	0.00020	0.1025	0.0028	0.7597	0.0909	629	17	360	278	628	16	175
P2-22	651	114	0.18	62	0.00039	0.1006	0.0014	0.8337	0.0548	618	8	608	141	618	8	102
P2-23	231	152	0.66	40	0.00001	0.1584	0.0038	1.5772	0.0897	948	21	992	103	950	21	96
P2-24	496	261	0.53	78	0.00008	0.1504	0.0026	1.4681	0.0758	903	15	951	98	904	15	95
P2-25	228	108	0.47	27	0.00013	0.1127	0.0055	0.9372	0.0931	688	32	616	185	686	31	112
P2-26	904	528	0.58	236	0.00045	0.2335	0.0024	3.8161	0.1197	1353	12	1934	52	1934	52	70
P2-27	142	60	0.42	16	0.00001	0.1138	0.0023	0.9892	0.0468	695	13	710	88	695	13	98
P2-28	811	307	0.38	91	0.00067	0.1192	0.0016	1.1682	0.0634	726	9	959	108	728	9	76
P2-29	149	87	0.58	20	0.00047	0.1316	0.0029	1.1121	0.1126	797	17	650	221	796	17	123
P2-30	233	200	0.86	26	0.00015	0.1009	0.0031	0.8138	0.0800	620	18	547	209	619	18	113
P2-31	133	156	1.18	19	0.00069	0.1223	0.0049	1.0759	0.2129	744	28	736	460	744	28	101
P2-32	365	550	1.51	43	0.00001	0.0909	0.0047	0.7343	0.0489	561	28	552	79	560	26	102
P2-33	304	248	0.81	52	0.00008	0.1529	0.0056	1.4928	0.0956	917	31	952	102	920	30	96
P2-34	404	367	0.91	65	0.00021	0.1416	0.0060	1.3246	0.0808	854	34	864	83	855	31	99
P2-35	726	398	0.55	76	0.00034	0.0992	0.0035	0.8270	0.0538	610	21	620	113	610	20	98
P2-36	60	86	1.45	12	0.00028	0.1631	0.0070	1.6058	0.2283	974	39	970	292	974	38	100
P2-37	354	357	1.01	39	0.00001	0.0958	0.0013	0.7516	0.0328	590	8	487	90	589	8	121
P2-38	174	111	0.64	31	0.00017	0.1665	0.0023	1.6902	0.1769	993	13	1031	221	993	13	96
P2-39	106	78	0.74	37	0.00042	0.3075	0.0080	5.0714	0.4866	1728	40	1951	169	1740	38	89
P2-40	456	130	0.28	50	0.00021	0.1119	0.0014	1.0053	0.0608	684	8	780	126	684	8	88
P2-41	469	279	0.59	78	0.00005	0.1559	0.0017	1.5585	0.0600	934	9	1001	74	935	9	93
P2-42	214	165	0.77	25	0.00016	0.1046	0.0020	0.8583	0.0729	641	12	587	184	641	12	109
P2-44	121	147	1.22	14	0.00001	0.0967	0.0029	0.7909	0.0463	595	17	579	105	594	17	103
P2-45	529	446	0.84	59	0.00006	0.0989	0.0019	0.8609	0.0579	608	11	712	138	609	11	85
P2-46	131	201	1.53	30	0.00001	0.1728	0.0054	1.8539	0.1274	1027	30	1142	119	1034	29	90
P2-47	186	232	1.25	20	0.00105	0.0899	0.0029	0.6838	0.1422	555	17	418	418	555	17	133
P2-48	494	374	0.76	81	0.00080	0.1473	0.0057	1.3191	0.1573	886	32	773	246	884	32	115
P2-49	237	38	0.16	24	0.00001	0.1059	0.0031	0.8955	0.0506	649	18	650	100	649	18	100

P2-50	367	194	0.53	53	−0.00005	0.1381	0.0032	1.3582	0.0447	834	18	967	43	854	17	86
P2-51	232	163	0.70	32	0.00008	0.1256	0.0025	1.1693	0.0652	763	14	853	107	764	14	89
P2-53	102	88	0.86	21	0.00001	0.1789	0.0040	1.7650	0.1121	1061	22	973	120	1058	22	109
P2-55	315	523	1.66	61	0.00045	0.1421	0.0022	1.4215	0.1245	856	13	1002	181	857	12	86
P2-56	105	157	1.49	14	0.00001	0.1097	0.0034	0.9285	0.0714	671	20	653	149	671	20	103
P2-58	425	230	0.54	40	0.00074	0.0914	0.0021	0.7500	0.1267	564	12	587	404	564	12	96
P2-59	59	59	1.01	8	0.00107	0.1176	0.0047	0.7719	0.2054	717	27	80	763	716	27	895
P2-60	137	94	0.68	21	0.00017	0.1428	0.0028	1.2755	0.0944	860	16	768	153	859	15	112
P2-61	309	148	0.48	34	0.00010	0.1069	0.0016	0.8899	0.0481	655	9	617	112	654	9	106
UI4-1	467	261	0.56	49	0.00001	0.0991	0.0019	0.8256	0.0470	609	11	619	114	609	11	98
UI4-2	147	183	1.24	31	0.00013	0.1700	0.0043	1.7041	0.1304	1012	24	1006	147	1012	24	101
UI4-3	213	332	1.56	24	0.00039	0.0862	0.0028	0.6399	0.0995	533	16	363	362	533	16	147
UI4-4	355	27	0.07	35	0.00001	0.1074	0.0018	0.9243	0.0330	658	10	688	64	658	10	96
UI4-5	340	481	1.42	35	0.00008	0.0816	0.0011	0.6949	0.0531	506	6	666	166	506	6	76
UI4-6	252	103	0.41	23	0.00034	0.0914	0.0036	0.7928	0.1214	564	21	706	338	564	21	80
UI4-7	335	259	0.77	61	0.00059	0.1567	0.0030	1.5911	0.1109	938	17	1032	137	940	16	91
UI4-8	174	31	0.18	26	0.00018	0.1576	0.0049	1.3475	0.1323	943	27	674	204	939	27	140
UI4-10.1	183	216	1.18	108	0.00008	0.4614	0.0145	11.1560	0.4676	2446	64	2609	41	2562	34	94
UI4-10.3	676	362	0.54	160	0.00014	0.2173	0.0042	1.7299	0.0634	1267	22	2488	28	2488	28	97
UI4-11	270	309	1.15	55	0.00001	0.1671	0.0031	5.5843	0.4989	996	17	992	48	996	16	97
UI4-12	472	332	0.70	88	0.00001	0.1697	0.0029	5.1223	0.4387	1011	16	1039	63	1012	15	100
UI4-13	68	66	0.98	28	−0.00027	0.3395	0.0162	0.9280	0.0452	1884	79	1946	130	1901	67	100
UI4-14	58	45	0.78	22	0.00013	0.3300	0.0138	4.7601	0.2552	1838	67	1842	132	1839	60	101
UI4-14.2	589	116	0.20	182	0.00067	0.3190	0.0060	4.8865	0.1298	1785	30	1770	90	1784	28	51
UI4-15	539	213	0.40	58	0.00026	0.1088	0.0018	0.4836	0.0454	666	11	669	97	666	10	45
UI4-16	394	453	1.15	48	0.00015	0.1027	0.0031	0.8686	0.0533	630	18	652	111	631	18	97
UI4-17	32	9	0.28	5	0.00063	0.1759	0.0094	1.6549	0.4992	1044	52	876	755	1044	51	119
UI4-18	7572	1490	0.20	128	0.00833	0.0171	0.0003	0.1758	0.0217	109	2	1056	264	1056	264	10
UI4-19	181	407	2.26	45	0.00064	0.1702	0.0041	1.4921	0.1807	1013	23	728	266	1011	23	139
UI4-20	231	148	0.64	26	0.00001	0.1043	0.0026	0.8473	0.0492	640	15	563	111	638	15	114
UI4-21	344	186	0.54	38	0.00001	0.1047	0.0021	0.8529	0.0337	642	12	570	71	640	12	113
UI4-22	119	83	0.70	23	0.00001	0.1740	0.0041	1.7228	0.1342	1034	23	980	152	1033	22	106
UI4-23	424	90	0.21	59	0.00007	0.1442	0.0033	1.3562	0.0884	868	19	876	125	868	19	99
UI4-24	230	200	0.87	28	0.00020	0.1103	0.0022	0.8835	0.1020	675	13	533	264	674	13	127
UI4-25	102	34	0.34	12	0.00117	0.1207	0.0056	0.8473	0.2365	734	32	238	779	734	32	309
UI4-26	1484	668	0.45	446	0.00011	0.2616	0.0042	6.2534	0.1478	1498	22	2591	26	2591	26	58
UI4-27	412	257	0.62	44	0.00011	0.1007	0.0024	0.8963	0.0553	618	14	760	118	620	14	81
UI4-28	222	190	0.86	35	0.00001	0.1374	0.0069	1.3490	0.1120	830	39	964	128	841	38	86
UI4-29.1	84	74	0.88	12	0.00001	0.1274	0.0049	1.0950	0.1031	773	28	685	184	771	28	113
UI4-29.2	365	71	0.20	36	−0.00022	0.1031	0.0023	1.0093	0.0848	633	13	957	169	635	13	66
UI4-30	554	167	0.30	74	0.00008	0.1338	0.0018	1.2615	0.0594	809	10	881	93	810	10	92
UI4-31	381	292	0.77	46	0.00017	0.1118	0.0026	0.9715	0.0578	683	15	710	114	684	15	96
UI4-32	239	196	0.82	31	0.00028	0.1203	0.0023	1.0901	0.0694	732	13	798	128	733	13	92
UI4-33	225	78	0.35	26	−0.00013	0.1103	0.0022	0.9793	0.0680	674	13	755	142	675	13	89
UI4-34	197	249	1.27	25	0.00001	0.1033	0.0015	0.9100	0.0547	634	9	739	124	634	9	86
UI4-35	142	118	0.83	48	0.00004	0.2854	0.0044	4.2675	0.1921	1619	22	1773	76	1631	21	91
UI4-35.2	368	143	0.49	31	0.00001	0.1048	0.0013	0.8854	0.0302	1865	19	1867	34	1865	16	99
UI4-36	290	244	0.66	137	0.00001	0.3354	0.0038	5.2803	0.1220	642	8	649	66	643	8	100
UI4-36	60	29	0.49	7	0.00001	0.1135	0.0028	0.9888	0.0665	693	16	715	132	693	16	97
UI4-37	246	206	0.84	46	0.00009	0.1661	0.0025	1.6372	0.0588	990	14	972	64	990	13	102
UI4-37.2	182	26	0.14	26	0.00019	0.1517	0.0035	1.4897	0.0993	911	20	963	127	912	20	95
UI4-38	44	42	0.95	8	0.00001	0.1594	0.0051	1.6362	0.1260	953	28	1054	139	957	28	90
UI4-39	223	357	1.60	32	−0.00009	0.1093	0.0016	0.9086	0.0380	668	9	615	83	668	9	109

Appendix 1. Continued.

						Radiogenic ratios				Age (Ma)						
Grain. Spot no.	U (ppm)	Th (ppm)	Th/U	Pb* (ppm)	$^{204}Pb/^{206}Pb$	$^{206}Pb/^{238}U$	±	$^{207}Pb/^{235}U$	±	$^{206}Pb/^{238}U$	±	$^{207}Pb/^{206}Pb$	±	W.M.† age	±	% discord
UI4-40	109	136	1.25	18	0.00030	0.1333	0.0024	1.2192	0.1297	807	14	817	230	807	14	99
UI4-41	141	118	0.84	60	0.00016	0.3686	0.0057	6.3894	0.2556	2023	27	2039	63	2025	25	99
UI4-41.2	306	304	0.99	43	0.00459	0.1511	0.0080	1.1088	0.3718	907	45	338	974	906	45	268
UI4-43	159	18	0.11	16	0.00044	0.1071	0.0025	0.7834	0.1558	656	14	330	390	656	14	199
UI4-44	342	110	0.32	38	0.00001	0.1109	0.0027	0.9696	0.0378	678	16	721	60	681	15	94
UI4-45	422	268	0.63	77	−0.00006	0.1686	0.0026	1.7120	0.0698	1004	14	1032	74	1005	14	97
UI4-45.2	401	532	1.33	62	0.00023	0.1175	0.0018	1.2253	0.1061	716	10	1086	177	717	10	66
UI4-47	135	144	1.06	18	0.00013	0.1094	0.0022	0.9597	0.0840	670	13	728	186	670	13	92
UI4-48	195	237	1.21	84	0.00001	0.3442	0.0064	5.3480	0.1564	1907	31	1843	38	1882	24	104
UI4-49	87	188	2.16	13	0.00028	0.1046	0.0033	0.8345	0.1601	642	19	524	469	641	19	123
UI4-50	92	69	0.76	11	0.00001	0.1083	0.0025	0.9405	0.1008	663	15	709	233	663	15	94
UI4-51	209	247	1.19	26	−0.00012	0.1025	0.0037	0.8587	0.0809	629	21	631	189	629	21	100
UI4-52	1291	781	0.61	91	0.00035	0.0631	0.0014	0.6415	0.0297	394	8	1036	79	1036	79	38
UI4-53	180	139	0.77	21	0.00001	0.1038	0.0015	0.9243	0.0381	637	9	761	80	638	9	84
UI4-54	342	260	0.76	73	0.00008	0.1925	0.0057	2.0507	0.1284	1135	31	1129	106	1134	30	101
UI4-55	137	98	0.71	15	0.00048	0.1031	0.0035	0.8323	0.1220	633	20	550	335	632	20	115
UI4-56	290	165	0.57	31	0.00008	0.1034	0.0016	0.8281	0.0502	634	9	533	130	634	9	119
UI4-57	130	169	1.30	30	0.00020	0.1812	0.0076	1.8029	0.1887	1074	42	990	197	1070	41	108
UI4-57.2	189	216	1.14	39	0.00007	0.1732	0.0031	1.6897	0.0929	1030	17	950	106	1028	17	108
UI4-59	126	230	1.84	19	−0.00018	0.1082	0.0028	0.9916	0.1056	662	16	821	224	663	16	81
UI4-60	122	91	0.74	14	0.00031	0.1049	0.0025	0.9145	0.1077	643	15	717	258	643	15	90
UI4-61	125	100	0.80	49	−0.00012	0.3390	0.0074	5.5109	0.1893	1882	36	1925	43	1899	28	98
US2-1	223	62	0.28	27	−0.00009	0.1244	0.0025	1.1094	0.0678	756	15	765	121	756	15	99
US2-3	226	275	1.21	29	0.00001	0.1057	0.0024	0.9082	0.0563	648	14	684	122	648	14	95
US2-4	385	20	0.05	40	0.00048	0.1128	0.0018	0.8655	0.0774	689	10	439	204	688	10	157
US2-5	125	53	0.42	14	0.00001	0.1152	0.0036	0.9250	0.0542	703	21	539	103	696	21	131
US2-6	154	45	0.29	18	0.00059	0.1231	0.0019	0.9798	0.1280	748	11	520	308	748	11	144
US2-7	164	155	0.94	18	0.00001	0.0978	0.0030	0.8091	0.0494	601	18	604	109	602	18	100
US2-9	77	82	1.07	7	0.00001	0.0800	0.0033	0.6647	0.0648	496	20	613	191	497	20	81
US2-10	238	69	0.29	130	0.00001	0.5051	0.0071	12.4740	0.2581	2636	30	2645	23	2641	18	100
US2-11	460	159	0.35	79	0.00042	0.1690	0.0018	1.8317	0.0737	1007	10	1163	76	1009	10	87
US2-12	138	116	0.84	18	0.00001	0.1150	0.0022	1.0260	0.0805	702	13	764	163	702	13	92
US2-13	12	0	0.02	1	−0.00231	0.0959	0.0057	1.2010	0.2278	591	34	1442	371	598	34	41
US2-14	43	0	0.01	4	0.00001	0.1019	0.0040	0.9406	0.0946	625	24	837	194	628	23	75
US2-15	230	97	0.42	23	0.00014	0.0998	0.0032	0.8490	0.0862	613	19	664	211	613	19	92
US2-16	301	154	0.51	52	0.00001	0.1655	0.0016	1.6335	0.0403	987	9	974	44	987	9	101
US2-16.2	113	42	0.37	20	0.00001	0.1700	0.0048	1.7196	0.0883	1012	26	1025	82	1013	25	99
US2-17	151	135	0.89	17	0.00011	0.1007	0.0079	0.8203	0.0952	618	47	571	174	615	45	108
US2-18	630	1115	1.77	190	0.01287	0.2015	0.0042	3.2355	0.3046	1183	22	1902	170	1902	170	62
US2-19	262	190	0.72	32	0.00001	0.1089	0.0025	0.9396	0.0506	666	15	694	101	667	15	96
US2-20	85	13	0.15	10	0.00001	0.1240	0.0035	1.1798	0.1036	753	20	900	173	755	20	84
US2-21	195	113	0.58	35	0.00021	0.1697	0.0032	1.7585	0.1120	1010	18	1073	122	1011	17	94
US2-22	74	37	0.50	11	−0.00061	0.1402	0.0038	1.4376	0.2407	846	22	1052	366	846	22	80
US2-23	132	56	0.42	14	0.00001	0.1069	0.0044	0.8872	0.0763	655	26	610	160	654	25	107
US2-24	780	260	0.33	79	0.00001	0.1016	0.0016	0.8469	0.0360	624	9	620	83	624	9	101
US2-26	201	183	0.91	19	0.00047	0.0826	0.0039	0.5927	0.1326	512	23	287	425	511	23	178
US2-27.1	112	79	0.70	15	0.00001	0.1199	0.0037	1.0527	0.0687	730	21	731	119	730	21	100
US2-27.2	257	103	0.40	30	0.00001	0.1130	0.0018	0.9852	0.0345	690	10	716	64	691	10	96

US2-28	165	167	1.01	19	0.00030	0.0974	0.0027	0.7225	0.0886	599	16	363	285	598	16	165
US2-29	201	75	0.37	27	0.00001	0.1320	0.0033	1.1972	0.0748	799	19	799	118	799	18	100
US2-30	262	168	0.64	30	0.00017	0.1083	0.0019	0.8733	0.0690	663	11	547	172	663	11	121
US2-31	86	40	0.47	48	0.00037	0.5079	0.0133	12.0100	0.4589	2648	57	2572	42	2599	34	103
US2-32	72	66	0.91	8	−0.00059	0.0980	0.0044	0.8616	0.2867	603	26	733	733	603	26	82
US2-33	56	19	0.34	7	0.00050	0.1307	0.0050	1.0589	0.3320	792	29	559	559	791	29	142
US2-34	548	152	0.28	86	0.00001	0.1578	0.0021	1.5878	0.0392	944	12	1014	39	950	11	93
US2-34.2	541	113	0.21	85	0.00007	0.1616	0.0027	1.6136	0.0527	965	15	998	54	968	14	97
US2-35	165	46	0.28	17	0.00001	0.1066	0.0027	0.9467	0.0523	653	15	756	101	655	15	86
US2-36	104	12	0.12	11	0.00001	0.1081	0.0031	0.9098	0.0677	662	18	641	147	661	18	103
US2-37	314	237	0.76	30	0.00001	0.0880	0.0023	0.6733	0.0525	544	13	431	165	543	13	126
US2-38	351	258	0.74	186	0.00018	0.4440	0.0049	11.0520	0.2391	2369	22	2658	29	2658	29	89
US38.2	517	656	1.27	304	0.00096	0.4489	0.0082	10.9700	0.3490	2391	36	2627	40	2627	40	91
US2-39	321	279	0.87	64	0.00007	0.1760	0.0029	1.8205	0.0750	1045	16	1070	74	1046	15	98
US2-40	120	266	2.22	13	0.00042	0.0755	0.0058	0.4858	0.1405	469	35	34	813	468	35	1399
US2-41	622	750	1.21	315	0.00246	0.3899	0.0089	9.4028	0.3840	2122	42	2605	53	2605	53	82
US2-42	284	105	0.37	39	0.00110	0.1379	0.0027	1.2269	0.1147	833	15	759	200	832	15	110
US2-43	151	134	0.89	47	0.00427	0.2408	0.0108	4.2920	1.2323	1391	56	2089	593	1397	56	67
US2-44	246	51	0.21	28	0.00025	0.1164	0.0028	1.0957	0.0759	710	16	877	134	712	16	81
US2-45	305	188	0.62	42	0.00018	0.1293	0.0037	1.1329	0.0757	784	21	726	126	782	21	108
US2-46	207	118	0.57	36	0.00001	0.1630	0.0027	1.6576	0.0730	974	15	1035	80	976	15	94
US2-47	78	63	0.81	8	0.00001	0.0964	0.0054	0.7319	0.0727	594	32	414	178	588	31	143
US2-48.1	315	389	1.23	66	0.00035	0.1675	0.0034	1.7154	0.1433	998	19	1049	167	999	19	95
US2-48.2	530	205	0.39	83	0.00179	0.1533	0.0030	1.6551	0.1324	919	17	1155	157	922	16	80
US2-49	472	326	0.69	54	0.00009	0.1048	0.0011	0.9563	0.0314	643	7	811	63	645	7	79
US2-50	315	227	0.72	106	0.00641	0.2655	0.0124	9.7716	0.8534	1518	64	3288	111	3288	111	46
US2-51	119	72	0.61	17	−0.00022	0.1352	0.0034	1.3909	0.0856	817	19	1058	111	825	19	77
US2-52	268	191	0.71	36	0.00001	0.1238	0.0025	1.0823	0.0490	752	14	722	83	751	14	104
US2-53	389	63	0.16	42	0.00001	0.1130	0.0022	0.9701	0.0357	690	13	684	63	690	13	101
US2-54	272	323	1.19	34	0.00046	0.0995	0.0022	1.0401	0.1405	612	13	1090	287	613	13	56
US2-55	259	163	0.63	34	−0.00008	0.1223	0.0023	1.1447	0.0673	744	13	866	115	745	13	86
US2-56	136	194	1.43	30	−0.00011	0.1722	0.0050	1.7825	0.1007	1024	28	1071	93	1028	27	96
US2-57	299	177	0.59	39	0.00832	0.1217	0.0030	1.1444	0.2672	740	17	875	564	740	17	85
US2-58	222	93	0.42	26	0.00016	0.1174	0.0025	0.9273	0.1198	715	14	503	301	715	14	142
US2-59	173	169	0.98	35	0.00033	0.1735	0.0069	1.7808	0.1757	1031	38	1054	182	1032	37	98
US2-60	980	270	0.28	73	0.01253	0.0757	0.0045	0.7355	0.2982	471	27	941	941	471	27	50
US2-61	80	54	0.67	14	−0.00024	0.1619	0.0039	1.5563	0.0820	967	22	920	93	965	21	105
US2-62	92	256	2.78	56	0.00001	0.3756	0.0107	6.1698	0.3443	2056	50	1943	82	2025	43	106
US2-63	96	70	0.72	11	0.00001	0.1104	0.0029	0.8008	0.0746	675	17	313	209	673	17	216
D2-1	786	69	0.09	72	0.00014	0.0985	0.0015	0.8076	0.0322	605	9	585	78	605	9	104
D2-2	310	189	0.61	35	0.00009	0.1075	0.0030	0.9247	0.0784	658	18	687	172	659	18	96
D2-3	151	147	0.97	17	0.00072	0.0968	0.0017	0.7164	0.1200	596	10	357	357	595	10	167
D2-4	233	103	0.44	25	0.00001	0.1052	0.0022	0.8747	0.0548	645	13	614	128	645	12	105
D2-5	210	227	1.08	25	0.00001	0.1017	0.0022	0.8047	0.0491	624	13	507	125	623	13	123
D2-6	636	1985	3.12	69	0.00067	0.0777	0.0017	0.6933	0.1023	482	10	765	335	483	10	63
D2-7	282	352	1.25	35	0.00014	0.1023	0.0020	0.8170	0.0703	628	12	528	189	627	12	119
D2-8.1	345	344	1.00	37	−0.00013	0.0952	0.0021	0.8334	0.0703	586	12	725	176	587	12	81
D2-9.1	262	265	1.01	51	0.00009	0.1699	0.0025	1.6484	0.1108	1012	14	939	137	1011	14	108
D2-10	486	337	0.69	93	0.00004	0.1753	0.0078	1.7950	0.1007	1041	43	1049	60	1044	35	99
D2-11	336	448	1.33	64	0.00014	0.1551	0.0040	1.4922	0.1036	929	22	922	131	929	22	101
D2-12	658	193	0.29	69	0.00012	0.1098	0.0021	0.9210	0.0637	672	12	634	144	671	12	106
D2-13	241	271	1.12	29	0.00001	0.0986	0.0022	0.8317	0.0426	606	13	646	95	607	13	94
D2-14	302	360	1.19	193	0.00001	0.4987	0.0086	12.0480	0.3058	2608	37	2608	28	2608	22	100

Appendix 1. Continued.

						Radiogenic ratios				Age (Ma)						
Grain. Spot no.	U (ppm)	Th (ppm)	Th/U	Pb* (ppm)	$^{204}Pb/^{206}Pb$	$^{206}Pb/^{238}U$	±	$^{207}Pb/^{235}U$	±	$^{206}Pb/^{238}U$	±	$^{207}Pb/^{206}Pb$	±	W.M.† age	±	% discord
D2-16	166	118	0.71	20	−0.00028	0.1077	0.0047	0.9767	0.0925	659	28	799	174	663	27	83
D2-17.1	300	152	0.51	27	0.00013	0.0944	0.0017	0.7777	0.0602	581	10	595	166	581	10	98
D2-19	154	96	0.63	18	0.00066	0.1110	0.0024	0.9870	0.1014	678	14	758	221	679	14	90
D2-20	169	506	2.99	29	0.00001	0.1024	0.0028	0.8695	0.0722	629	16	659	170	629	16	95
D2-21	70	48	0.69	8	0.00061	0.1085	0.0042	0.8376	0.3437	664	25	452	1293	664	25	147
D2-22	184	224	1.22	149	0.00004	0.6120	0.0095	21.2350	0.4427	3078	38	3195	19	3171	17	96
D2-23	411	295	0.72	60	0.00003	0.1347	0.0025	1.2393	0.0762	814	14	830	122	815	14	98
D2-23.2	1207	963	0.80	37	0.00169	0.0305	0.0008	0.3178	0.0283	194	5	1085	173	1085	173	18
D2-24	58	64	1.10	11	0.00041	0.1660	0.0066	1.6101	0.2615	990	36	938	349	990	36	106
D2-25	190	107	0.56	31	0.00015	0.1538	0.0037	1.4921	0.1476	922	21	939	203	922	21	98
D2-26	597	728	1.22	260	0.00015	0.3722	0.0053	8.8875	0.1877	2040	25	2589	23	2589	23	79
D2-27	1053	1214	1.15	85	0.00076	0.0753	0.0012	0.7149	0.0621	468	7	894	183	469	7	52
D2-28	959	399	0.42	101	0.00071	0.1104	0.0015	1.4209	0.0736	675	9	1495	94	1495	94	45
D2-29	309	391	1.27	42	−0.00020	0.1083	0.0022	1.0196	0.0557	663	13	877	103	666	13	76
D2-31	110	62	0.56	13	0.00072	0.1177	0.0034	0.8351	0.2759	717	19	262	994	717	19	274
D2-34	241	138	0.57	36	0.00001	0.1467	0.0026	1.5071	0.0515	882	14	1056	56	893	14	84
D2-35	460	633	1.38	35	0.00049	0.0767	0.0092	0.6964	0.1237	476	55	802	267	490	54	59
D2-36	608	715	1.18	56	0.00045	0.0903	0.0011	0.8458	0.0628	558	7	865	156	558	7	64
D2-37	693	435	0.63	71	0.00062	0.1008	0.0016	1.0974	0.0891	619	10	1171	162	619	10	53
D2-37.2	904	934	1.03	63	0.00040	0.0671	0.0008	0.6886	0.0455	419	5	1054	134	1054	134	40
D2-39	322	125	0.39	22	0.00036	0.0713	0.0012	0.6260	0.1020	444	8	730	381	444	7	61
D2-40	173	55	0.32	20	0.00111	0.1147	0.0025	1.0273	0.1358	700	15	772	294	700	15	91
D2-41	434	615	1.42	53	0.00672	0.1063	0.0029	1.0151	0.2359	651	17	906	556	652	17	72
D2-42	180	119	0.66	33	0.00015	0.1745	0.0025	1.6126	0.1037	1037	14	838	132	1035	14	124
D2-44	398	124	0.31	44	−0.00006	0.1118	0.0013	0.9406	0.0563	683	8	639	128	683	8	107
D2-45	86	69	0.80	13	0.00001	0.1388	0.0040	1.2430	0.1534	838	23	772	266	838	23	109
D2-46	421	451	1.07	39	0.00030	0.0893	0.0021	0.7243	0.0673	551	12	560	202	552	12	98
D2-47	407	223	0.55	155	0.00010	0.3549	0.0062	8.9867	0.2427	1958	29	2686	31	2686	31	73
D2-48	48	26	0.54	6	0.00064	0.1117	0.0048	0.9856	0.3174	683	28	741	741	683	28	92
D2-49	345	336	0.97	59	0.00007	0.1486	0.0019	1.4481	0.0703	893	11	948	95	894	11	94
D2-50	48	71	1.47	7	−0.00068	0.1066	0.0047	1.0225	0.2861	653	27	917	687	653	27	71
D2-51	559	97	0.17	48	0.00001	0.0907	0.0011			560	7	770	72	562	6	73
D2-52	516	332	0.64	93	0.00011	0.1684	0.0033	0.8115	0.0301	1003	18	996	83	1003	18	101
D2-52.2	383	643	1.68	72	0.00016	0.1533	0.0175	1.5023	0.1881	919	98	960	84	943	64	96
D2-53	79	49	0.62	15	0.00001	0.1786	0.0050	1.6627	0.1046	1059	27	855	114	1048	27	124
D2-54	267	490	1.84	28	0.00024	0.0988	0.0018	1.0219	0.0745	608	10	1068	144	608	10	57
D2-55	123	121	0.98	15	0.00001	0.1066	0.0026	0.9531	0.1344	653	15	770	316	653	15	85
D2-56	247	99	0.40	46	0.00010	0.1826	0.0032	1.9189	0.0853	1081	17	1100	80	1082	17	98
D2-57	637	751	1.18	72	0.00036	0.1019	0.0028	1.0000	0.0531	625	16	963	89	625	16	65
D2-58	144	64	0.44	15	0.00020	0.1002	0.0020	0.8327	0.0815	615	12	615	215	615	12	100
D2-59	180	65	0.36	24	0.00009	0.1331	0.0038	1.3879	0.0933	806	22	1085	119	815	21	74
D2-60.2	470	303	0.64	40	0.00023	0.0829	0.0011	0.6433	0.0421	513	6	464	145	513	6	111
D2-61	272	274	1.01	33	0.00001	0.1047	0.0018	0.8802	0.0522	642	10	638	122	642	10	101
D2-62	139	92	0.66	15	0.00001	0.1031	0.0015	0.8880	0.0543	632	9	691	128	633	9	92
D2-63	234	92	0.39	28	0.00012	0.1232	0.0022	1.0952	0.0491	749	13	757	84	749	13	99
D2-64	154	115	0.75	31	0.00001	0.1805	0.0035	1.8603	0.0935	1070	19	1062	91	1069	19	101

†The ages given in the last columns are based on the weighted mean of the $^{207}Pb/^{206}Pb$ and $^{206}Pb/^{238}U$ ages of each grain. For discordant zircons with MSWD > 10, the $^{206}Pb/^{238}U$ age was used when it was less than 800 Ma, whereas the $^{207}Pb/^{206}Pb$ age was used for zircons with $^{206}Pb/^{238}U$ ages older than 800 Ma, and these were always assumed to be minimum crystallization ages.

Appendix 2. U-Pb geochronology data for detrital zircons separated from Cambrian sandstone in Israel (Elat area)

						Radiogenic ratios				Age (in Ma)						
Grain Spot no.	U (ppm)	Th (ppm)	Th/U	Pb* (ppm)	$^{204}Pb/^{206}Pb$	$^{206}Pb/^{238}U$	±	$^{207}Pb/^{235}U$	±	$^{206}Pb/^{238}U$	±	$^{207}Pb/^{206}Pb$	±	W.M.† age	±	% discord
K2-1.1	309	261	0.84	33	0.00001	0.0933	0.0030	0.7836	0.0340	575	18	636	55	581	17	90.4
K2-2.1	102	71	0.70	12	0.00001	0.1078	0.0037	0.9528	0.0450	660	22	746	61	670	21	88.4
K2-3.1	87	23	0.27	8	0.00001	0.0969	0.0043	0.8290	0.0520	596	25	677	87	602	24	88.1
K2-4.1	143	73	0.51	14	0.00023	0.0916	0.0030	0.7432	0.0707	565	18	561	198	565	18	100.7
K2-5.1	299	176	0.59	34	0.00008	0.1067	0.0031	0.8707	0.0383	654	18	573	65	648	17	114
K2-7.1	100	48	0.48	11	0.00009	0.1092	0.0042	0.9393	0.0602	668	25	688	102	669	24	97.2
K2-8.1	296	128	0.43	29	−0.00008	0.0952	0.0028	0.7948	0.0383	586	16	623	78	587	16	94
K2-9.1	669	316	0.47	38	0.00278	0.0580	0.0017	0.4357	0.0452	364	11	390	230	364	11	93.3
K2-10.1	206	93	0.45	20	−0.00006	0.0939	0.0029	0.7367	0.0359	578	17	489	78	574	17	118.4
K2-11.1	130	75	0.57	12	0.00023	0.0879	0.0028	0.7612	0.0400	543	16	703	84	549	16	77.3
K2-12.1	178	110	0.62	17	0.00001	0.0880	0.0028	0.7201	0.0469	544	17	580	119	545	17	93.8
K2-13.1	841	547	0.65	42	0.00465	0.0481	0.0016	0.4710	0.0781	303	10	958	362	304	10	31.6
K2-14.1	170	116	0.68	28	0.00010	0.1509	0.0048	1.4814	0.0822	906	27	964	88	911	26	94
K2-15.1	381	90	0.24	39	0.00005	0.1058	0.0033	0.9267	0.0386	648	19	727	51	658	18	89.2
K2-16.1	288	210	0.73	30	−0.00002	0.0930	0.0031	0.7601	0.0365	573	18	578	68	573	17	99.1
K2-17.1	179	67	0.37	17	−0.00016	0.0964	0.0020	0.7895	0.0538	593	12	581	141	593	12	102.1
K2-18.1	98	61	0.62	13	0.00014	0.1258	0.0030	1.0513	0.0651	764	17	626	122	761	17	122.1
K2-19.1	336	170	0.51	34	−0.00006	0.0964	0.0013	0.8120	0.0329	593	8	643	80	594	8	92.3
K2-20.1	556	239	0.43	61	0.00001	0.1064	0.0018	0.8820	0.0290	652	10	608	58	651	10	107.2
K2-21.1	495	460	0.93	41	0.00362	0.0757	0.0015	0.6274	0.1051	470	9	608	400	470	9	77.4
K2-22.1	154	89	0.58	17	0.00011	0.1051	0.0014	0.8149	0.0366	644	8	462	94	643	8	139.6
K2-23.1	315	155	0.49	42	0.00001	0.1314	0.0036	1.1124	0.0723	796	21	654	124	792	21	121.7
K2-24.1B	254	101	0.40	25	0.00001	0.0969	0.0019	0.8132	0.0331	596	11	634	74	597	11	94.1
K2-25.1	190	87	0.46	18	−0.00005	0.0886	0.0025	0.8475	0.0648	547	15	910	145	551	15	60.1
K2-26.1B	111	111	1.00	13	−0.00016	0.0954	0.0020	0.8170	0.0697	588	12	677	181	588	12	86.8
K2-26.2	160	155	0.97	15	0.00001	0.0791	0.0031	0.6211	0.0430	491	18	489	121	491	18	100.4
K2-27.1	265	60	0.23	146	0.00001	0.5129	0.0213	12.7820	0.6987	2669	91	2660	52	2662	45	100.4
K2-28.1	150	85	0.57	19	−0.00004	0.1178	0.0027	1.0025	0.0503	718	15	664	93	717	15	108.1
K2-29.1	71	22	0.31	7	−0.00009	0.1058	0.0021	0.8917	0.0392	648	12	643	81	648	12	100.8
K2-30.1	354	309	0.87	68	0.00004	0.1674	0.0019	1.6552	0.0325	998	10	978	31	996	10	102
K2-31.1	344	444	1.29	40	0.00001	0.0923	0.0013	0.7809	0.0252	569	8	653	60	570	8	87.1
K2-32.1	698	359	0.51	71	0.00049	0.0990	0.0029	0.8020	0.0371	609	17	557	72	606	17	109.2
K2-33.1	140	47	0.33	15	−0.00013	0.1035	0.0024	0.8933	0.0529	635	14	696	115	636	14	91.2
K2-34.1	164	126	0.77	62	0.00001	0.3258	0.0038	4.9143	0.0759	1818	19	1789	16	1801	12	101.6
K2-34.2	63	62	0.98	45	0.00001	0.1009	0.0031	0.8166	0.0279	1760	33	1804	91	1765	31	97.6
K2-36.1	281	146	0.52	30	−0.00003	0.1018	0.0012	0.8450	0.0273	625	7	612	63	625	7	102.2
K2-37.1	72	59	0.83	9	0.00003	0.1113	0.0033	0.9429	0.0487	680	19	655	85	679	19	103.8
K2-38.1	167	58	0.35	16	−0.00001	0.0954	0.0015	0.7937	0.0214	587	9	617	45	588	9	95.2
K2-39.1	283	176	0.62	29	0.00002	0.0949	0.0031	0.7866	0.0402	584	18	608	78	585	18	96.1
K2-40.1	328	282	0.86	37	0.00005	0.0995	0.0064	0.8313	0.0639	611	38	625	77	614	34	97.7
K2-41.1	537	163	0.30	51	0.00017	0.0964	0.0025	0.8128	0.0375	593	15	644	77	595	15	92.1
K2-42.1	67	64	0.97	9	0.00010	0.1157	0.0036	0.9959	0.0585	706	21	688	102	705	21	102.6
K2-43.1	243	108	0.45	145	0.00044	0.5297	0.0049	13.4470	0.1910	2740	21	2690	16	2708	13	101.8
K2-43.3	590	139	0.24	349	0.00631	0.4914	0.0189	14.0670	1.8713	2577	82	2887	214	2617	77	89.2
K2-44.1	207	165	0.80	23	−0.00011	0.0996	0.0026	0.8136	0.0448	612	15	576	102	611	15	106.2
K2-45.1	29	27	0.93	3	0.00041	0.1009	0.0030	0.7608	0.1420	620	18	400	400	620	18	155

Appendix 2. Continued.

						Radiogenic ratios				Age (in Ma)						
Grain Spot no.	U (ppm)	Th (ppm)	Th/U	Pb* (ppm)	$^{204}Pb/^{206}Pb$	$^{206}Pb/^{238}U$	±	$^{207}Pb/^{235}U$	±	$^{206}Pb/^{238}U$	±	$^{207}Pb/^{206}Pb$	±	W.M.† age	±	% discord
K15-2.1	522	390	0.75	196	−0.00001	0.3263	0.0086	5.3199	0.1481	1820	42	1930	12	1922	11	94.3
K15-4.1	210	39	0.18	25	0.00003	0.1236	0.0035	1.0879	0.0430	751	20	737	53	749	19	101.9
K15-5.1	361	53	0.15	34	0.00009	0.0983	0.0039	0.8366	0.0570	604	23	666	112	607	23	90.8
K15-6.1	54	39	0.73	10	0.00001	0.1615	0.0061	1.6959	0.1388	965	34	1099	143	973	33	87.9
K15-7.1	163	7	0.04	17	−0.00010	0.1078	0.0034	1.4191	0.0903	660	20	1538	100	660	20	42.9
K15-8.1	514	405	0.79	60	0.00015	0.1032	0.0031	0.8426	0.0335	633	18	575	51	627	17	110.2
K15-9.1	284	57	0.20	32	0.00001	0.1161	0.0033	0.9821	0.0343	708	19	653	36	695	17	108.5
K15-10.1	318	121	0.38	32	−0.00005	0.0980	0.0030	0.8220	0.0387	603	18	633	71	605	17	95.2
K15-11.1	250	148	0.59	26	−0.00003	0.0981	0.0032	0.8433	0.0350	603	18	687	49	614	17	87.8
K15-12.1	471	268	0.57	66	0.00001	0.1305	0.0042	1.2341	0.0466	791	24	886	34	822	20	89.3
K15-13.1	416	214	0.51	38	−0.00006	0.0866	0.0034	0.7285	0.0429	535	20	640	86	541	20	83.6
K15-15.1	95	71	0.75	15	0.00069	0.1486	0.0075	1.4835	0.1355	893	42	997	150	901	41	89.5
K15-16.1	54	60	1.12	7	0.00016	0.1108	0.0041	0.9602	0.0736	677	24	703	139	678	24	96.3
K15-17.1	316	196	0.62	33	0.00002	0.1144	0.0017	0.9598	0.0244	698	10	635	41	695	10	110
K15-18.1	524	265	0.51	42	0.00112	0.0920	0.0046	0.7011	0.0730	567	27	424	202	564	27	133.6
K15-19.1	501	207	0.41	152	0.00000	0.3181	0.0037	4.6947	0.1102	1780	18	1750	35	1774	16	101.8
K15-20.1	200	160	0.80	22	0.00009	0.1221	0.0018	1.1091	0.0327	743	10	803	51	745	10	92.5
K15-21.1	329	215	0.66	48	0.00005	0.1585	0.0018	1.4715	0.0333	948	10	848	38	942	10	111.8
K15-22.1	313	146	0.47	97	0.00005	0.3261	0.0040	5.0560	0.1125	1819	20	1839	31	1825	17	98.9
K15-23.1	557	774	1.39	49	−0.00002	0.0967	0.0026	0.7951	0.0271	595	15	590	40	595	14	100.9
K15-24.1	764	329	0.43	53	0.00208	0.0822	0.0006	0.7091	0.0348	509	4	694	105	509	4	73.3
K15-25.1	170	75	0.13	39	0.00107	0.0747	0.0017	0.6598	0.0448	1149	31	1047	57	1126	27	109.8
K15-26.1	265	122	0.46	25	−0.00006	0.1047	0.0022	0.8797	0.0303	642	13	636	54	642	12	100.9
K15-27.1	180	247	1.38	17	0.00007	0.1018	0.0027	0.8725	0.0546	625	16	680	118	626	16	91.9
K15-28.1	244	246	1.01	29	0.00002	0.1300	0.0019	1.1618	0.0282	788	11	768	37	786	11	102.6
K15-29.1	170	38	0.22	16	−0.00007	0.1064	0.0017	0.8582	0.0437	652	10	549	104	651	10	118.8
K15-31.1	88	28	0.32	7	0.00001	0.0883	0.0021	0.7742	0.0459	546	13	727	112	548	13	75
K15-32.1	186	65	0.35	17	0.00009	0.0988	0.0208	0.7893	0.1786	607	##	528	139	572	92	115.1
K15-33.1	496	191	0.39	37	0.00087	0.0830	0.0110	0.8108	0.1392	514	66	952	203	556	63	54
K15-34.1	106	117	1.11	10	−0.00013	0.1057	0.0025	0.9089	0.0755	648	14	687	173	648	14	94.3
K15-35.1	98	33	0.34	9	−0.00031	0.1011	0.0032	0.8896	0.1504	621	19	736	387	621	19	84.3
K15-37.1	107	40	0.38	13	0.00012	0.1227	0.0023	1.0299	0.0498	746	13	634	94	744	13	117.7
K15-38.1	188	136	0.72	21	−0.00004	0.1001	0.0018	0.8572	0.0315	615	10	678	66	617	10	90.8
K15-39.1	449	203	0.45	40	0.00268	0.0825	0.0058	0.8471	0.6151	511	34	1053	###	511	34	48.5
K15-40.1	400	135	0.34	41	0.00002	0.1025	0.0013	0.8294	0.0192	629	8	555	40	627	7	113.3
K15-41.1	295	93	0.32	27	0.00007	0.0919	0.0019	0.7472	0.0256	567	11	567	55	567	11	100
K15-42.1	103	35	0.34	11	−0.00004	0.1007	0.0021	0.8639	0.0342	618	12	682	68	620	12	90.7
K15-43.1	152	121	0.79	18	−0.00010	0.1031	0.0036	0.8739	0.0558	633	21	656	110	633	20	96.5
K15-45.1	1188	671	0.57	293	0.00122	0.1989	0.0096	4.9906	0.3466	1170	52	2671	75	2671	75	43.8
K15-45.2	1696	725	0.43	167	0.00344	0.0893	0.0025	1.8577	0.1093	552	15	2355	86	2355	86	23.4
K15-46.1	250	148	0.59	44	0.00003	0.1636	0.0034	1.5744	0.0495	977	19	922	44	968	17	105.9
K15-47.1	75	50	0.66	14	−0.00001	0.1707	0.0055	1.6909	0.0817	1016	30	981	67	1010	28	103.6
K15-48.1	317	119	0.38	33	0.00006	0.1036	0.0017	0.8499	0.0435	635	10	586	105	635	10	108.4
K15-49.1	270	97	0.36	32	0.00001	0.1162	0.0016	0.9997	0.0264	709	9	687	46	708	9	103.1
K15-50.1	92	87	0.94	11	0.00001	0.0961	0.0071	0.7862	0.0900	591	42	580	182	591	41	101.9
K15-51.1	121	54	0.45	12	0.00006	0.0979	0.0022	0.7628	0.0483	602	13	472	130	601	13	127.5
K15-52.1	300	177	0.59	28	0.00014	0.0875	0.0022	0.7531	0.0360	541	13	689	82	544	13	78.5
K15-53.1	346	176	0.51	39	0.00006	0.1082	0.0013	0.8807	0.0222	662	8	569	46	660	7	116.5

K15-54.1	260	136	0.52	38	0.00003	0.1389	0.0025	1.2244	0.0434	838	14	740	62	834	14	113.3
K15-55.1	89	58	0.65	17	0.00008	0.1722	0.0037	1.7827	0.0657	1024	20	1071	56	1030	19	95.7
K15-56.1	109	56	0.51	85	0.00001	0.6593	0.0131	21.1260	0.6332	3264	51	3069	32	3069	33	106.4
K15-56.2	247	19	0.08	134	−0.00001	0.5189	0.0088	13.7530	0.3161	2694	37	2761	23	2743	19	97.6
K15-57.1	243	155	0.64	26	0.00001	0.0989	0.0021	0.8077	0.0283	608	13	576	55	606	12	105.6
K15-58.1	305	181	0.59	59	0.00017	0.1790	0.0030	1.9668	0.0499	1062	17	1189	34	1189	34	89.3
K15-58.2	630	165	0.26	53	0.00131	0.0867	0.0013	0.7886	0.0874	536	8	805	244	536	8	66.5
K15-59.1	355	176	0.50	32	0.00073	0.0874	0.0016	0.6835	0.0440	540	10	482	137	540	10	112.1
K15-60.1	2593	773	0.30	131	0.00667	0.1790	0.0030	1.9668	0.0499	1062	17	1189	34	1189	34	18.4
K15-61.1	178	494	2.78	32	0.00001	0.0874	0.0016	0.6835	0.0440	540	10	482	137	540	10	109
K5-1.1	279	165	0.59	28	0.00458	0.0963	0.0030	0.8097	0.0429	593	18	639	86	595	18	92.8
K5-3.1	276	71	0.26	31	0.00005	0.1162	0.0034	0.9883	0.0353	708	20	664	37	698	18	106.7
K5-4.1	120	98	0.81	36	0.00023	0.2580	0.0098	3.8998	0.1753	1479	50	1794	36	1794	36	82.5
K5-5.1	102	63	0.62	10	0.00005	0.0914	0.0039	0.7559	0.0744	564	23	602	191	565	23	93.6
K5-6.1	352	298	0.85	37	0.00001	0.0944	0.0028	0.7840	0.0380	582	17	611	77	583	17	95.1
K5-7.1	347	65	0.19	31	−0.00004	0.0937	0.0030	0.7779	0.0320	577	18	611	48	581	17	94.6
K5-8.1	488	167	0.34	51	−0.00004	0.1043	0.0028	0.8730	0.0303	640	17	629	40	638	16	101.7
K5-9.1	251	230	0.92	30	0.00001	0.1041	0.0030	0.8734	0.0367	638	18	634	59	638	17	100.7
K5-10.1	414	246	0.59	46	0.00001	0.1041	0.0031	0.8654	0.0369	639	18	614	59	637	17	104.1
K5-11.1	312	140	0.45	32	−0.00002	0.0968	0.0027	0.8248	0.0299	596	16	667	43	605	15	89.3
K5-12.1	265	140	0.53	28	0.01179	0.0997	0.0027	0.8312	0.0335	613	16	620	59	613	15	98.8
K5-14.1	277	565	2.04	39	0.00033	0.0946	0.0033	0.7980	0.0362	583	19	646	56	590	18	90.2
K5-15.1	672	549	0.82	276	0.00216	0.3401	0.0111	7.6501	0.2988	1887	54	2489	30	2489	30	75.8
K5-16.1	988	495	0.50	142	0.00023	0.1381	0.0038	1.9959	0.0940	834	21	1711	66	1711	66	48.7
K5-16.2	509	303	0.59	130	0.00004	0.2406	0.0078	3.5745	0.1475	1390	41	1762	40	1762	40	78.9
K5-17.1	104	54	0.52	11	−0.00001	0.1041	0.0023	0.8444	0.0492	638	13	561	116	637	13	113.8
K5-18.1	157	151	0.96	21	0.00060	0.1114	0.0020	0.9252	0.0318	681	12	611	59	678	12	111.4
K5-18.2	189	110	0.58	31	0.00001	0.1510	0.0024	1.4212	0.0462	906	13	877	56	905	13	103.4
K5-20.1	388	317	0.82	41	0.00052	0.0929	0.0024	0.7615	0.0264	572	14	584	43	573	13	98
K5-21.1	73	44	0.60	7	0.00010	0.0977	0.0021	0.6800	0.0805	601	12	216	244	600	12	278
K5-22.1	75	55	0.74	10	0.00002	0.1241	0.0029	1.1084	0.0597	754	17	766	99	754	17	98.4
K5-23.1	104	26	0.25	14	−0.00004	0.1322	0.0031	1.1659	0.0426	801	18	740	54	795	17	108.2
K5-24.1	257	59	0.23	25	−0.00001	0.0981	0.0012	0.8391	0.0326	603	7	676	78	604	7	89.2
K5-25.1	149	107	0.72	17	−0.00006	0.1053	0.0024	0.8778	0.0304	645	14	621	52	643	14	104
K5-26.2	129	40	0.31	14	0.00013	0.1049	0.0026	0.9116	0.0442	643	15	709	85	645	15	90.7
K5-27.1	299	46	0.15	30	0.02851	0.1072	0.0019	0.8800	0.0381	657	11	586	83	656	11	112
K5-29.1	169	253	1.49	23	−0.00011	0.1076	0.0024	1.1231	0.1591	659	14	1088	303	660	14	60.6
K5-30.1	198	80	0.40	25	−0.00004	0.1235	0.0023	1.1581	0.0583	751	13	869	95	753	13	86.4
K5-31.1	170	58	0.34	21	0.00001	0.1217	0.0034	1.1696	0.0742	740	20	919	114	745	20	80.6
K5-32.1	156	192	1.23	18	0.00001	0.0903	0.0038	0.7957	0.0468	557	22	738	80	570	21	75.5
K5-33.1	87	37	0.43	40	−0.00002	0.4117	0.0118	9.5821	0.3339	2223	54	2546	28	2546	28	87.3
K5-33.2	185	175	0.94	95	0.00000	0.4226	0.0092	10.5700	0.3220	2272	42	2666	31	2666	31	85.2
K5-33.3	205	77	0.38	117	−0.00018	0.5146	0.0081	12.6190	0.2607	2676	35	2633	19	2643	17	101.6
K5-34.1	305	493	1.62	37	0.00001	0.0898	0.0039	0.7860	0.0722	554	23	726	169	557	23	76.4
K5-35.1	134	75	0.56	14	0.00005	0.0953	0.0032	0.8250	0.0620	587	19	701	140	589	19	83.6
K5-36.1	104	40	0.39	11	0.00015	0.1013	0.0022	0.8289	0.0335	622	13	580	71	621	13	107.3
K5-37.1	373	399	1.07	163	−0.00001	0.3575	0.0234	8.1077	0.5483	1970	##	2502	19	2502	19	78.7
K5-37.2	469	168	0.36	242	0.00005	0.4704	0.0039	11.2830	0.1205	2485	17	2596	10	2596	10	95.7
K5-37.3	131	115	0.87	65	0.00009	0.4080	0.0093	9.5019	0.3237	2206	43	2547	38	2547	38	86.6
K5-38.1	335	237	0.71	56	0.00740	0.1598	0.0023	1.6587	0.0541	956	13	1076	56	962	13	88.8
K5-39.1	186	262	1.41	35	0.00001	0.1480	0.0032	1.5008	0.0465	890	18	1029	40	1029	40	86.4
K5-40.1	423	319	0.75	54	0.00002	0.1174	0.0029	1.1935	0.0510	716	17	1034	66	716	17	69.2

Appendix 2. Continued.

Grain Spot no.	U (ppm)	Th (ppm)	Th/U	Pb* (ppm)	$^{204}Pb/^{206}Pb$	Radiogenic ratios				Age (in Ma)						
						$^{206}Pb/^{238}U$	±	$^{207}Pb/^{235}U$	±	$^{206}Pb/^{238}U$	±	$^{207}Pb/^{206}Pb$	±	W.M.† age	±	% discord
K5-41.1	331	265	0.80	56	0.00795	0.1484	0.0017	1.4794	0.0338	892	9	995	38	897	9	89.6
K5-43.1	204	260	1.28	32	−0.00004	0.1239	0.0020	1.1443	0.0307	753	12	838	41	760	12	89.8
K5-44.1	140	104	0.74	22	−0.00005	0.1429	0.0019	1.2874	0.0419	861	11	786	60	859	11	109.6
K5-45.1	165	35	0.21	17	−0.00006	0.1060	0.0019	0.8963	0.0303	650	11	650	58	650	11	99.9
K5-46.1	77	62	0.80	9	0.00012	0.1004	0.0033	0.8029	0.0540	617	19	529	125	615	19	116.5
K5-47.1	231	101	0.44	21	0.00014	0.0884	0.0012	0.7283	0.0249	546	7	595	66	547	7	91.8
K5-48.1	387	34	0.09	42	0.00001	0.1176	0.0013	0.9948	0.0246	717	8	651	45	715	8	110.1
K5-49.1	196	296	1.51	124	0.00030	0.4551	0.0041	11.0210	0.1833	2418	18	2612	22	2612	22	92.6
K5-49.2	207	281	1.36	109	0.00001	0.3905	0.0078	9.0201	0.2615	2125	36	2533	32	2533	32	83.9
K5-50.1	223	48	0.22	37	0.00006	0.1713	0.0016	1.5962	0.0269	1019	9	856	27	856	27	119
K5-50.2	629	13	0.02	68	0.00092	0.1180	0.0024	1.0187	0.0382	719	14	696	62	718	14	103.3
K5-51.1	951	50	0.05	75	0.00024	0.0850	0.0008	0.7129	0.0284	526	5	632	83	526	5	83.2
K5-52.1	614	259	0.42	55	−0.00021	0.0887	0.0022	0.7699	0.0310	548	13	708	62	555	13	77.3
K5-53.1	142	340	2.40	20	−0.00002	0.0905	0.0015	0.7564	0.0338	558	9	626	87	559	9	89.2
K5-54.1	159	105	0.66	21	0.00011	0.1277	0.0032	1.1069	0.0374	775	18	703	42	764	17	110.2
K5-55.1	237	233	0.98	37	−0.00004	0.1383	0.0026	1.2830	0.0434	835	14	847	55	836	14	98.6
K5-56.1	136	81	0.60	21	0.00135	0.1444	0.0031	1.4348	0.0555	870	17	987	62	878	16	88.1
K5-57.1	709	1200	1.69	152	0.00029	0.1670	0.0013	2.3966	0.0577	995	7	1698	41	1698	41	58.6
K5-57.2	500	772	1.54	148	−0.00007	0.2254	0.0068	3.1638	0.1127	1310	36	1657	30	1657	30	79.1
K5-58.1	178	122	0.69	19	−0.00028	0.0988	0.0028	0.8560	0.0601	607	16	704	136	608	16	86.3
K5-59.1	30	12	0.40	4	0.00003	0.1386	0.0059	1.4292	0.2071	837	34	1063	294	840	33	78.7
K5-60.1	295	155	0.53	52	0.00001	0.1660	0.0053	1.6836	0.0642	990	30	1030	35	1007	22	96.1
K5-60.2	623	275	0.44	107	0.00001	0.1644	0.0045	1.6632	0.0491	981	25	1024	16	1012	13	95.8
K5-61.1	151	90	0.60	54	0.00031	0.3217	0.0101	5.2242	0.2094	1798	50	1923	39	1876	30	93.5
K5-61.2	267	32	0.12	33	−0.00003	0.1302	0.0040	1.4698	0.0688	789	23	1243	63	789	23	63.4
K5-62.1	186	199	1.07	38	0.00011	0.1659	0.0057	1.7432	0.0929	989	32	1101	75	1006	29	89.8
K5-62.2	172	149	0.86	31	−0.00008	0.1596	0.0050	1.6134	0.0678	954	28	1023	50	971	24	93.2
K5-63.1	145	81	0.56	15	0.00005	0.0962	0.0028	0.7849	0.0461	592	16	573	107	592	16	103.3
K5-63.2	223	128	0.58	21	0.00001	0.0882	0.0035	0.7483	0.0375	545	21	657	55	559	20	83
K5-64.1	185	64	0.32	32	0.00001	0.1564	0.0046	1.6015	0.0682	592	27	497	112	587	27	119.2
K5-64.2	199	119	0.64	19		0.0963	0.0047	0.7584	0.0553	937	26	1049	56	956	23	89.3
K20-1.1	567	115	0.20	54	0.00006	0.0941	0.0027	0.7579	0.0325	580	16	545	64	578	16	106.3
K20-2.1	84	77	0.92	15	0.00008	0.0963	0.0030	0.8097	0.0429	593	18	639	86	595	18	92.8
K20-4.1	632	550	0.87	60	0.00001	0.1162	0.0034	0.9883	0.0353	708	20	664	37	698	18	106.7
K20-5.1	158	83	0.52	18	0.00005	0.2580	0.0098	3.8998	0.1753	1479	50	1794	36	1794	36	82.5
K20-6.1	670	29	0.04	58	0.00023	0.0914	0.0039	0.7559	0.0744	564	23	602	191	565	23	93.6
K20-7.1	1996	956	0.48	86	0.00005	0.0944	0.0028	0.7840	0.0380	582	17	611	77	583	17	95.1
K20-8.1	183	122	0.67	26	0.00001	0.0937	0.0030	0.7779	0.0320	577	18	611	48	581	17	94.6
K20-9.1	681	393	0.58	73	−0.00004	0.1043	0.0028	0.8730	0.0303	640	17	629	40	638	16	101.7
K20-10.1	437	121	0.28	40	−0.00004	0.1041	0.0030	0.8734	0.0367	638	18	634	59	638	17	100.7
K20-11.1	538	109	0.20	54	0.00001	0.1041	0.0031	0.8654	0.0369	639	18	614	59	637	17	104.1
K20-12.1	324	164	0.51	36	0.00001	0.0968	0.0027	0.8248	0.0299	596	16	667	43	605	15	89.3
K20-13.1	181	86	0.47	18	−0.00002	0.0997	0.0027	0.8312	0.0335	613	16	620	59	613	15	98.8
K20-15.1	85	47	0.55	12	0.00006	0.0946	0.0033	0.7980	0.0362	583	19	646	56	590	18	90.2
K20-16.1	21	13	0.59	3	0.00033	0.3401	0.0111	7.6501	0.2988	1887	54	2489	30	2489	30	75.8
K20-17.1	231	187	0.81	25	0.00216	0.1381	0.0038	1.9959	0.0940	834	21	1711	66	1711	66	48.7
K20-18.1	283	492	1.74	56	0.00001	0.0933	0.0030	0.7836	0.0340	575	18	636	55	581	17	90.4

K20-19.1	202	142	0.71	124	0.00001	0.1078	0.0037	0.9528	0.0450	660	22	746	61	670	21	88.4
K20-20.1	211	116	0.55	34	0.00001	0.0969	0.0043	0.8290	0.0520	596	25	677	87	602	24	88.1
K20-21.1	293	208	0.71	30	0.00023	0.0916	0.0030	0.7432	0.0707	565	18	561	198	565	18	100.7
K20-22.1	253	250	0.99	46	0.00008	0.1067	0.0031	0.8707	0.0383	654	18	573	65	648	17	114
K20-24.1	118	60	0.50	13	0.00009	0.1092	0.0042	0.9393	0.0602	668	25	688	102	669	24	97.2
K20-25.1	55	112	2.01	9	−0.00008	0.0952	0.0028	0.7948	0.0383	586	16	623	78	587	16	94
K20-27.1	231	69	0.30	24	−0.00006	0.0939	0.0029	0.7367	0.0359	578	17	489	78	574	17	118.4
K20-28.1	500	99	0.20	60	0.00023	0.0879	0.0028	0.7612	0.0400	543	16	703	84	549	16	77.3
K20-29.1	198	224	1.13	24	0.00001	0.0880	0.0028	0.7201	0.0469	544	17	580	119	545	17	93.8
K20-31.1	320	173	0.54	39	0.00010	0.1509	0.0048	1.4814	0.0822	906	27	964	88	911	26	94
K20-32.1	200	110	0.55	25	0.00005	0.1058	0.0033	0.9267	0.0386	648	19	727	51	658	18	89.2
K20-32.2	143	140	0.98	20	−0.00002	0.0930	0.0031	0.7601	0.0365	573	18	578	68	573	17	99.1
K20-34.1	293	96	0.33	37	−0.00001	0.3263	0.0086	5.3199	0.1481	1820	42	1930	12	1922	12	94.3
K20-36.1	1008	1862	1.85	45	0.01136	0.0591	0.0036	0.6141	0.2394	370	22	1079	###	370	22	34.3
K20-37.1	136	93	0.68	17	0.00003	0.1236	0.0035	1.0879	0.0430	751	20	737	53	749	19	101.9
K20-38.1	1247	201	0.16	72	0.00009	0.0983	0.0039	0.8366	0.0570	604	23	666	112	607	23	90.8
K20-39.1	242	122	0.51	23	0.00001	0.1615	0.0061	1.6959	0.1388	965	34	1099	143	972	33	87.9
K20-40.1	177	136	0.77	67	−0.00010	0.1078	0.0034	1.4191	0.0903	660	20	1538	100	660	20	42.9
K20-41.1	160	80	0.50	18	0.00015	0.1032	0.0031	0.8426	0.0335	633	18	575	51	627	17	110.2
K20-42.1	126	107	0.85	21	0.00001	0.1161	0.0033	0.9821	0.0343	708	19	653	36	696	17	108.5
K20-43.1	150	179	1.20	21	−0.00005	0.0980	0.0030	0.8220	0.0387	603	18	633	71	605	17	95.2
K20-44.1	164	54	0.33	72	−0.00003	0.0981	0.0032	0.8433	0.0350	603	18	687	49	613	17	87.8
K20-45.1	761	662	0.87	51	0.00001	0.1305	0.0042	1.2341	0.0466	791	24	886	34	823	20	89.3
K20-46.1	82	22	0.26	9	−0.00006	0.0866	0.0034	0.7285	0.0429	535	20	640	86	540	19	83.6
K20-48.1	119	77	0.64	16	−0.00006	0.1196	0.0046	1.0031	0.0736	728	26	633	131	724	26	115.1
K20-49.1	665	1636	2.46	190	0.00019	0.1825	0.0022	1.8196	0.0456	1080	12	995	43	1074	12	108.6
K20-50.1	158	125	0.79	21	0.00013	0.1190	0.0016	0.9920	0.0380	725	9	620	76	724	9	117
K20-51.1	220	125	0.57	98	0.00000	0.3983	0.0059	6.6665	0.1364	2161	27	1977	22	1977	22	109.3
K20-52.1	182	50	0.28	24	−0.00003	0.1345	0.0020	1.1502	0.0314	813	12	675	45	804	12	120.4
K20-53.1	70	84	1.19	9	0.00001	0.1070	0.0026	0.8401	0.0406	655	15	489	88	650	15	134.1
K20-54.1	67	42	0.63	8	0.00046	0.1151	0.0045	0.8666	0.1140	702	26	396	296	700	26	177.3
K20-55.1	438	306	0.70	57	0.00007	0.1197	0.0026	0.9750	0.0430	729	15	571	80	724	15	127.7
K20-56.1	88	77	0.88	20	0.00012	0.1940	0.0048	1.8966	0.0793	1143	26	955	64	1116	24	119.7
K20-57.1	213	136	0.64	133	0.00000	0.5325	0.0111	12.0350	0.3247	2752	47	2497	25	2497	25	110.2
K20-57.2	1641	829	0.50	217	0.02156	0.1252	0.0024	2.2526	0.2659	761	14	2104	215	2104	215	36.1
K20-58.1	385	167	0.43	48	0.00004	0.1215	0.0011	1.0220	0.0222	739	6	639	41	737	6	115.6
K20-59.1	218	150	0.69	29	0.00001	0.1213	0.0016	1.0248	0.0261	738	9	650	44	734	9	113.6
K20-60.1	288	312	1.09	163	0.00003	0.4468	0.0067	10.3980	0.2214	2381	30	2546	23	2546	23	93.5
K20-61.1	176	85	0.49	22	0.00012	0.1220	0.0031	0.9927	0.0534	742	18	567	99	736	18	130.9

†The ages given in the last columns are based on the weighted mean of the $^{207}Pb/^{206}Pb$ and $^{206}Pb/^{238}U$ ages of each grain. For discordant zircons with MSWD > 10, the $^{206}Pb/^{238}U$ age was used when it was less than 800 Ma, whereas the $^{207}Pb/^{206}Pb$ age was used for zircons with $^{206}Pb/^{238}U$ ages older than 800 Ma, and these were always assumed to be minimum crystallization ages.